Atf5 Links Olfactory Receptor Induced Stress Response to Proper Neuronal Function

Jerome Keoki Kahiapo

Submitted in partial fulfillment of the
requirements for the degree of
Doctor of Philosophy
under the Executive Committee
in the Graduate School of Arts and Sciences

COLUMBIA UNIVERSITY

2020

Abstract

Atf5 Links Olfactory Receptor Induced Stress Response to Proper Neuronal Function

Jerome Keoki Kahiapo

Mammalian olfaction requires the enduring expression of a single olfactory receptor (OR) gene for the life of each sensory neuron. This is due to the fact that OR proteins play multiple roles in the coherent perception of odors, first by sensing molecular cues from the external environment, and by directing the wiring of neuronal projections faithfully from the peripheral sensory neurons to the brain. Both of these processes require singular and stable OR expression in olfactory sensory neurons (OSNs. The transcription factor Atf5 has previously been shown to enforce these modes of expression, through a process that requires the unfolded protein response (UPR). The work presented in this thesis deciphers how Atf5 enables proper OR expression and neuronal function in the olfactory system. We identify the developmental window in which UPR is activated, and provide evidence that Atf5 protein expression coincides with the assembly of a multi-chromosomal enhancer hub that drives singular and robust OR transcription, opposing a model in which precocious polygenic OR transcription initiates UPR. Further, we show that Atf5 directly regulates a collection of genes that facilitate proper OR trafficking, axonogenesis, as well as transcription factors and chromatin modifiers, which we propose to be involved in stable OR expression and neuronal maturation. Finally, we find that Atf5 has a special role in the olfactory system that cannot be replaced by its ubiquitously expressed homologue, Atf4, and that this is due to a requisite interaction between Atf5 and the bZIP transcription factor Cebpγ, and potentially other transcription factors known to be critical for olfactory function.

Table of Contents

List of Charts, Graphs, Illustrations

Acknowledgments

First, I'd like to thank all scientific mentors I've had through my life. As an undergraduate student, I studied philosophy, so my decision to pursue a professional scientific career path can best be described as quixotic. I first started in Alan Lau's lab, where I washed and autoclaved dishes, refilled pipette tip boxes (by hand!) and put that little cotton in the top of the serological pipettes. There I was first captivated by watching students running western blots, what I could have only thought was some sort of black magic. Intrigued, I then worked in Mariana Gerschenson's lab, where I was delighted to do actual science: qPCR every day. Next, I was lucky enough to join a stem cell themed Master's program and worked on a thesis with Robert Blelloch at UCSF, where I experienced the satisfaction of pursuing my own project, and the merit of good scientific thinking. These people have provided inspiration and encouragement, for which I will forever be indebted.

Of course, I must thank Stavros. Stavros, I've learned is quite atypical of a mentor. In large part, I think it is because he treats everyone as a peer, and therefore as equals. Still, he customizes his mentorship strategies for each individual in a way that is most fruitful for all. Two things that struck me when I first started working for him were 1) his possession of child-like appreciation of cool results and 2) his infuriating ability to make being a good scientist look so easy. At the same time, his refusal to be fastidious and his folksy demeanor reminded much (too much!) of myself.

Next, I would like the many colleagues I've had along my path to now, which numbers too many to name here. Obviously all the (past and present) members of the Lomvardas lab, who are all stimulating and accomplished scientific peers. Also, they all have been caring and generous friends.

Finally, I would like to thank my parents, who are not scientists but nonetheless have animated me along this path as much as anyone else. Their unwavering support (despite moving farther and farther away) as I pursue my academic goals has been paramount to my success. I will be thrilled when they stop asking me "…….so when are you graduating?".

Introduction

Mammalian Olfaction

Olfaction is a vital sensory modality that instructs critical aspects of animal behavior, which include finding appropriate food, avoiding predators, and identifying mates or kin. As a chemosensory system, it links the external chemical environment and our internal state, providing a representation of particular volatile chemicals, or odors, encountered, which in turn can elicit judgments and actions that can be innate or learned. The qualia of these representations form the sensation of smell.

In mammals, odors are detected by olfactory sensory neurons (OSNs) arranged in a pseudostratified fashion in the main olfactory epithelium (MOE), which lines the posterior recesses of the nasal cavity. OSNs extend dendrites apically toward the nasal mucosa, forming a platform for odorant detection. At the same time, OSN axons pierce the basal lamina of the neuroepithelium, fasciculate into nerve fibers, and coalesce into discrete glomerular structures in the olfactory bulb (OB), the first relay station for olfactory information from the MOE to the brain[1]. Glomeruli are synaptic-rich structures in the olfactory bulb that are innervated by projection neurons, including mitral and tufted cells, which project to a set of brain regions collectively called the olfactory cortex. These higher order regions include the piriform cortex, the entorhinal cortex, olfactory nucleus, olfactory tubercle and the amygdala, which perform distinct but integrative functions. Collectively, these higher brain regions process incoming information about complex odors and are responsible for such things as odor identification, discrimination, valence, as well as learning and memory of these sensory inputs[2–4]. Importantly, each glomerulus is composed of axonal projections from OSNs that are homogeneous in terms of olfactory receptor (OR) gene expression.

This generates a large collection of glomeruli on the OB that forms a map of axonal projections wherein stochastic and distributed OR expression among neurons in the MOE becomes sorted from the periphery to the brain. Thus, complex odors in the environment are recognized by OSNs expressing a particular set of OR genes, and this information is encoded by the set of glomeruli that represent these ORs. Because each mitral and tufted projection neuron innervates a single glomerulus, the pattern of glomerular activation, and thus OR representation, is retained as complex odor information is transmitted to higher brain regions.

In addition to the MOE, a number of parallel olfactory subsystems participate in communicating chemosensory information from the periphery to the brain. In the mouse, for example, the vomeronasal organ (VNO), a tubular structure that sits at the base of the anterior nasal septum, is responsible for the detection of pheromones, non-volatile semiochemicals that elicit innate behaviors. The VNO houses sensory neurons in a pseudostratified epithelial structure whose axons project to the posterior dorsal aspect of the OB. There, VNO axons converge into glomerular structures as well, analogous to the main olfactory system. In contrast though, VNO axons can innervate more than one glomerulus, and many glomeruli are heterogeneous in terms of receptor content[5–8]. And unlike the main olfactory system, VNO projections to the AOB are not as spatially stereotyped between individuals of the same species, as is the case for neurons of the MOE. VNO axons innervate second order projection neurons, mitral cells, which synapse with higher brain regions[9]. But as opposed to the wiring of the MOB, mitral cells of the AOB form dentritic contacts with multiple glomeruli[7]. Collectively, these differences in circuitry indicate an integrative property of sensory information in the vomeronasal sensory system at the level of the AOB that is absent in the main olfactory system, and emphasizes a difference in the logic of information processing between these two olfactory subsystems. Finally, unlike olfactory

information conveyed through the MOE, mitral cells of the AOB project to regions of the brain that are distinct from second order projections in the main olfactory system, including the vomeronasal amygdala, contributing to the innate social-sexual responses that result from pheromone detection in rodents.

The MOE exhibits regenerative potential throughout the animal's life that supports tissue homeostasis due to naturally occurring cell turnover, as well as the capacity to completely restore all cell types following various forms of acute injury[10]. Accordingly, the MOE contains a population of resident stem cells, the horizonal basal cells (HBCs), which line the basal layer of the epithelium and can both self-renew and differentiate. HBCs can be identified by a number of molecular markers, including ICAM-1 and Krt5[11], and fate mapping of HBCs reveal that in the native setting, these stem cells are largely quiescent, though at a basal levels, can give rise to a transit amplifying population, globose basal cells (GBCs)[10,12]. GBCs can be defined by the expression of the helix-loop-helix transcription factor Ascl1[13], are enriched for cell cycle markers[14], and divide asymmetrically to produce immediate neural progenitor cells (INPs)[15]. By lineage tracing, genetic ablation of Ascl1, and single cell RNA-seq, it has been shown that both HBCs and GBCs also contribute to non-neuronal lineages in the MOE[14,16,17], including the sustentacular cells[18] and microvillous cells[19]. In contrast, INPs can be defined by the expression of Ngn[13,20], and are restricted to the neuronal lineage, undergoing the last cell division before terminal maturation to OSNs[13,21,22]. DNA labelling techniques reveal the time course of development of the neuronal lineage: INP cells transition to immature OSNs (iOSNs) over the course of ~5 days, and then terminally differentiated mature OSNs (mOSNs) are observed ~5 days after that[23]. The lifespan of an mOSN has been reported to range from ~1-3 months[24], and is age[25] and activity dependent[26].

Olfactory Receptors Constitute a Large Gene Family and Exhibit Singular Expression

Olfactory receptors make up a family of G-protein coupled receptors (GPCRs) that are highly expressed in OSNs[27]. OR proteins are localized to the cell surface of olfactory cilia within the dendritic compartment of OSNs where they are exposed to odors present in the nasal cavity[28,29]. Upon ligand binding, OR proteins signal through the activation of heterotrimeric, olfactory-specific G_α subunit[30,31] ($G_\alpha$olf), which then stimulates Adenylyl Cyclase 3[32,33] (Adcy3). Subsequent cAMP production is coupled to the opening of a cyclic nucleotide-gated channel[34], resulting in neuronal depolarization. Mutations that ablate these components result in an anosmic phenotype as a result of reduced electrophysiological responses in olfactory neurons[30,32,35]. Thus, ORs are responsible for coupling the recognition of odors to the production of action potentials that signal to the brain through a cAMP-dependent signaling pathway.

One of the most striking features of the OR gene family is its size. In mice, for example, ~1400 genes encode for ORs[36,37], which group into ~70 genomic clusters scattered across nearly all chromosomes[36–39]. Collectively, OR gene clusters occupy 40 Mb of the mouse genome and are characterized by an unusually high AT content[37]. The genomic dominance of this gene family suggests an evolutionary "brute-force" strategy for odorant detection in which OR gene numbers have been greatly expanded in the course of evolution to accommodate the detection of a large number of potential odorant molecules[40,39].

As environmentally encountered odors are presented as a mixture of discrete odorant molecules, the breadth of chemical space recognized by the olfactory system is afforded by a large gene family with variable ligand binding specificities. In support of this, the binding preferences and affinities for specific ORs and discrete odors, as well as complex odor mixtures, has been

investigated in heterologous systems, as well as in vitro and in vivo models[41–45]. These results revealed that ORs can recognize a number of odors, and a specific odor can bind to a number of ORs, indicating that the perception of a complex odor is the resulting combination of OR activity. Additionally, modulatory effects on the response of specific ORs due to combinations of odors have been observed, initially for the rodent I7 receptor[46,47], and more recently using a high-throughput approach, as a widespread property of OR proteins[48]. These findings, coupled to the expansive OR repertoire represented in the MOE, highlights the immense discriminatory power of the olfactory apparatus.

ORs appear to be expressed in a stochastic, monogenic and monoallelic fashion. The stochastic nature of OR expression was quickly appreciated following the cloning of the first OR genes[27], allowing for the generation of RNA in-situ probes. Among the 5 million neurons of the adult mouse MOE, RNA probes designed against specific OR transcripts demonstrate that each OR is expressed in only a subset (~0.1%) of OSNs in a punctate, yet spatially restricted way[49–52] . This observation, coupled with the immense size of the gene family, suggests that each OSN expresses one or a small number of OR genes. Additionally, several lines of evidence support the model that ORs are expressed in a "singular" fashion. First, utilizing a PCR-based approach by cloning OR RNA from one or a small number of OSNs, the identity of specific ORs can be distinguished by the molecular weights of the products following restriction enzyme treatment[53]. By assessing the receptor content of single OSNs from rodents wherein the maternal and paternal alleles can be distinguished, only one OR allele is detected. Moreover, experiments in which two OR genes or two alleles of the same gene are genetically tagged by unique reporters fail to demonstrate co-expression of two ORs within the same neuron[54]. Finally, RNA/DNA FISH experiments reveal the exclusive transcription of only one OR allele within the nucleus[55].

While the notion of singular OR expression in OSNs has become canon in the field, these techniques cannot exhaustively rule out the possibility that some subset of neurons, or some particular set of ORs violate singular OR expression. More recently, single cell RNA-sequencing experiments have provided valuable insight into what has been hitherto a technically intractable question to address[14,56–58]. By these analyses, mature OSNs express at high frequency a single or dominant OR transcript. In contrast, in progenitor cells (GBCs, INPs) low level co-expression of multiple OR transcripts can be detected. These snapshots of the receptor content of many individual neurons at different developmental stages illustrate a trajectory for OSNs wherein stable, singular OR expression is preceded by precocious co-expression. The reasons why early co-expression of a handful of ORs is permitted (or required?), and how expression of a single OR ultimately dominates in mature OSNs remains unclear.

OR Identity Specifies Neuronal Function

Singular OR expression is crucial for the proper functioning of the olfactory system for two reasons. First, the identity of the chosen OR specifies the receptive field that will lead to OR-ligand binding and neuronal depolarization at dendritic termini. Analysis of ligand specificities for specific receptors has revealed that a given OR can bind to a number of odorant molecules, and that a given odorant molecule can activate a number of ORs[43,44]. Thus, while the expression of a large family of distinct OR proteins localized to the nasal mucosa accounts for the ability to recognize a vast set of odorants, the discrete expression of precisely one receptor in any individual neuron provides a strategy to distinguish among which particular odorant is encountered by virtue of the set of neurons, and accordingly, the set of glomeruli, that become activated.

A second aspect of the olfactory system which makes singular OR expression indispensable for coherent olfactory perception is that it is crucial for the proper targeting of OSNs to the brain. Neurons that express an identical OR project axons to ~2 discrete glomeruli on each half of the OB in a manner that is stereotyped among individuals within a species[59,60] The identity of the OR expressed plays an instructive role in the convergence of like neurons to the same glomeruli, as genetic manipulations that either swap OR identity or mutate OR protein at a targeted OR allele alter the targeting properties of the OSN[61–63]. Both OR mRNA and protein can be detected in the axonal termini of OSNs[28,60] and the mechanism that affords precise glomerular targeting among OSNs expressing the same OR seems to be temporally regulated during development, involving first an OR-independent stage that allows olfactory nerve fibers to project to the olfactory nerve layer, followed by an OR-dependent stage in which axons navigate the glomerular layer of the OB and converge to their proper targeting sites[23]. Corresponding spatial cues by way of the graded expression of targeting molecules regulate axonal projections along the dorsal-ventral axis from the MOE to the OB that is genetically programmed and independent of the expressed OR[64]. In contrast, both the basal, agonist-independent activity as well as the ligand-dependent activity of a particular OR protein play roles in axonal targeting along the anterior-posterior axis, as well as glomerular segregation of OSN axons, respectively. In this way, the identity of the chosen OR protein, through agonist dependent and independent signaling properties, allows the convergence of like-OSNs to discrete glomeruli, rendering each glomerulus homogeneous in terms of receptor content. Thus, each OR identity is represented into 2-4 stereotypic glomeruli in the OB, forming a topographic map of >3000 glomeruli: activation of distinct glomerular combinations by each odor is considered the basis of odor identification[60,65].

In summary, singular OR expression plays an integral role in the coherent perception of smell. Localization of OR proteins to both the dendritic and axonal compartments of OSNs links neuronal activation of a distributed set of neurons in the MOE driven by characteristic ligand-OR interactions, and the targeting of like neurons to a set of glomeruli in the OB. In this way, exposure to an odorant or set of odorants is faithfully represented by the set of OSNs and their corresponding glomeruli that become activated as a consequence, which then forms the basis for the activation of downstream neuronal signaling from projection neurons to deeper parts of the brain.

The Mechanism of Singular OR Expression

Considering the size of the OR gene family, limiting the expression of a single OR allele out of ~3000 potential "choices" poses a daunting regulatory challenge for olfactory neurons. In addition, given that singular OR expression is critical for coherent olfactory perception, the processes that regulate this mode of gene expression must be tightly tuned to ensure the fidelity and stability of singular OR expression. At the same time, the MOE is continuously regenerating throughout an animal's life, so the mechanisms that enforce singular OR expression coincident with OSN maturation must also be engaged and maintained throughout life.

Transcriptional singularity is accomplished by the coordinated function of superimposed regulatory mechanisms. First, singular OR expression is preceded by the global silencing of OR gene clusters by two potentially inter-dependent mechanisms. In the first case, OR genes become decorated by histone modifications usually reserved for constitutively inactive gene regions, namely H3K9me3 and H4K20me3[66]. These marks can be detected in the neuronal progenitor cells (INPs), and persist in mature OSNs, but are absent in the basal stem cell population (HBCs). At the same time, OSN nuclei adopt an atypical nuclear arrangement in which heterochromatic

genomic regions collapse to the center of the nucleus in a handful of chromocenters, wherein OR genes co-localize with heterochromatic markers, such as Heterochromatin Binding Protein 1 β (HP1β), and are largely excluded from regions of the nucleus enriched for euchromatic markers (e.g. PolII)[67]. This is coincident with the downregulation of Lamin B Receptor (LBR), which interacts with the nuclear envelope as well as HP1β. Thus, at early stages of OSN differentiation, OR genes become both physically and biochemically repressed, rendering them refractory to transcriptional activation.

The repressive constraints globally imposed on OR genes are critical for singular OR expression, and cis and trans factors have been identified that facilitate an escape from this state. Transgenic mice bearing OR "mini-genes" including as little as 300bp of promotor DNA driving a reporter construct is sufficient to recapitulate OR-like expression in the MOE[68]. Such transgenes and other meta analyses of OR promotor sequences[37,69] reveal enrichment for binding sites for homeodomain proteins, such as LHX2, as well as EBF family proteins, both of which have been implicated in OR expression and proper OSN development[70,71].

Considering the number and homogeneity of OR promotors, additional mechanisms are required to ensure stochastic and singular OR expression. Indeed, OR activation relies on OR enhancers, named Greek islands, which exhibit an OSN specific chromatin modification signature, bear stereotypically spaced LHX2 and EBF binding sites which are bound in vivo, and are proximal to OR clusters but remain intransigent to heterochromatin[72,73]. Currently ~60 Greek islands have been identified. Genetic manipulations demonstrate that Greek islands are necessary and sufficient for transcriptional activation of OR genes *in cis* [73,76]. Importantly, Greek islands coalesce in the nucleus into a multi-chromosomal hub that demonstrates high frequency interactions in mature OSNs that is significantly diminished in INP cells and absent in HBCs[73,76].

Underscoring the importance of the nuclear arrangement of OR genes in singular OR expression, Greek islands cover the transcriptionally active OR, spatially confining it into euchromatic territory[67,73,76]. This interaction is coincident with the absence of heterochromatic marks and the presence of a histone modification indicative of transcriptionally active genes, H3K4me3, on the chosen OR[66]. Thus, singular and robust OR transcription is accompanied by a series of layered processes involving the deposition of a heterochromatic epigenetic signature onto OR genes globally as well as the commissioning of multi-chromosomal Greek islands that converge on the transcriptionally active OR allele that allows it to defy spatial constraints imposed on the silenced OR genes.

OR-Elicited Feedback Reinforces Singular and Stable Expression

Mutually exclusive and enduring OR expression is promoted by both a feedback signal that prevents the transcriptional activation of additional ORs, and a feedforward signal that permits the sustained expression of the chosen OR. These two phenomena may be due to two independent mechanisms, or may be the result of a common mechanism. Evidence for feedback driving mutually exclusive OR expression was first supported by experiments in which mouse strains engineered to express a transgenic tetO-OR-GFP coupled with an OSN-specific driver failed to express both the ectopic and endogenous OR in the same OSN[77]. Further, mutant OR transgenes with deletions in the coding sequence, or that bear an OR coding sequence that can be transcribed but not translated, both lead to co-expression of the targeted mutation with additional ORs, indicating that the mechanism that precludes co-expression requires a translatable, intact OR coding sequence[75,78,77]. These mutant transgenes also demonstrate a targeting defect, in which

axons from neurons equipped with the mutant transgenes innervate the OB broadly, to multiple glomeruli, underlying the essential role of singular OR expression in proper axonal targeting.

Subsequently, the notion that OR stability is regulated by a signal established by the OR itself came from experiments utilizing lineage tracing strategies, in which transcriptional activation of a mutant or wild-type OR can drive expression of a Cre-recombinase and subsequent irreversible activation of an unlinked reporter allele. These studies reveal that neurons that had at one time activated transcription of the mutant OR extinguish its expression, while expressing other ORs[79]. This concept of "gene-switching" suggests that the process of OR choice is, at least during some window of development, a serial and not parallel process, during which properties of the chosen OR are vetted for "fitness". Failure to meet the necessary requirements (e.g. intact coding sequence, translatable protein) prevents stable expression of that OR and permits transcriptional activation of an additional one.

While the precise mechanisms that underlie feedback remain incompletely known, one critical component appears to be the dual function histone demethylase, Lsd1[80]. Lsd1 can demethylate both H3K9 and H3K4 mono- and di-methylated substrates in a context dependent manner, leading to both activating and repressive functions respectively. Because OR clusters become first globally silenced by the deposition of H3K9me3 marks before detectable OR expression, Lsd1 can act as a de-repressor of a chosen OR; at the same time, the subsequent removal of activating H3K4me3 marks will suppress expression of that OR. Thus, enduring OR expression can be achieved by the timely downregulation of Lsd1 immediately after fulfilling its role as a de-repressor. In support of this, Lsd1 is transiently expressed in neuronal progenitor cells and excluded from mature OSNs. Early deletion of Lsd1 leads to global loss of OR transcription, consistent with its involvement in OR de-repression, while ectopic expression of Lsd1 in mature

OSNs leads to unstable OR expression[81]. While it remains unknown how Lsd1 expression is extinguished following OR selection, several lines of evidence support the idea that Adcy3 acts as a sensor for OR expression that signals for Lsd1 downregulation. First, ectopic expression of an OR transgene in the context of a Lsd1 mutant strain (in which ORs are not expressed) is sufficient to rescue Adcy3 expression. Second, deletion of Adcy3 permits an expansion of Lsd1 expressing cells throughout the MOE. Finally, deletions of Adcy3 lead to reduced and unstable OR expression, as well as an axon targeting defect[82].

Thus, in addition to the spatial restrictions imposed by a Greek island hub in supporting singular OR expression, limiting enzymatic activity by critical chromatin modifying enzymes followed by their prompt transcriptional downregulation may cooperate as an orthogonal means by which singular and stable OR expression is ensured[83].

Atf5 Links OR induced UPR to Stabilize OR choice and OSN Maturation

During OSN development, Atf5 acts as a sensor for OR translation in the ER through the unfolded protein response (UPR)[84]. The UPR is a highly conserved cellular process that recognizes aberrant or pathological levels of unfolded proteins and leads to restorative or abortive measures to rectify it. To date, there are three known sensors of UPR stress in mammals: IRE1, Atf6 and Perk1. Although the signaling pathways utilized by these sensors can be outlined independently, their collective purpose is to 1) decrease protein folding load, 2) increase protein folding capacity, and/or 3) initiate apoptosis.

Atf5 is a stress response transcription factor that is highly expressed in OSNs[85]. Atf5, like its ubiquitously expressed paralogue Atf4, becomes transiently and preferentially translated in response to a number of sources of both endogenous and exogenous stress signals[86]. This is due to

the regulated phosphorylation of the translational initiation factor subunit eIF2α by a handful of known stress induced kinases (one of which is Perk1), which leads to limiting initiator $tRNA^{Met}$ levels. By modulating the concentration of $tRNA^{Met}$, ribosome scanning across mRNA molecules leads to a generalized reduction in translational engagement at canonical start codons. Instead, the presence of a cryptic upstream open reading frame (uORF) within the 5'UTR of the mRNAs for these stress response transcription factors allows for "skipping" of the cryptic uORF and re-engagement at a downstream start codon, leading to the preferential translation of these factors under stressed conditions[87].

The concept that OR translation in the ER is the signal for transient Atf5 translation is supported by two genetic observations. First, in a mutant mouse strain that does not express ORs due to an early conditional deletion of Lsd1, Atf5 protein is not detectable in the MOE[81]. Second, ectopic expression of a transgenic OR in the Lsd1 KO strain restores the transient translation of Atf5[84]. Furthermore, the role of UPR in transmitting this signal is demonstrated by targeted mutations of either Perk1, or of the requisite eIF2α phosphorylation site- in both cases, olfactory neurons fail to translate Atf5[84].

Currently, it is unknown how ORs induce UPR at all. One potential explanation is that the high transcriptional output of a selected OR is sufficient to overload the protein folding machinery, leading to ER stress. Alternatively, OR proteins may bear a molecular signature that can induce ER stress by directly engaging with molecular components of UPR machinery. Finally, OR proteins may require specific processing partners for proper folding and egress from the ER, which are initially absent at the onset of OR expression. In agreement with the third possibility, OR proteins are notoriously difficult to be expressed in heterologous systems, but candidate and cDNA

screening has identified a number of OSN specific chaperone proteins that can promote surface expression of OR protein, such as RTP1 and RTP2[88].

In order to decipher the role of Atf5 in stable OR selection and OSN maturation, clarity is needed regarding the timing of UPR induction, and the nature of the signal that initiates UPR. Recent single cell RNA-seq from MOE has provided evidence that, contrary to the "one-receptor one-neuron" rule of OR expression, multiple OR transcripts can be detected within a single OSN during an early developmental window[56,57,89]. While sequencing platforms and data processing pipelines vary among these reports, the upper limit for the number of ORs detected per cell has ranged from 9[56] to 20[89]. Consistently, these investigations have found that polygenic OR expression is synchronous with the onset of OR transcription during a precursor, or progenitor stage of OSN development, and that once these cells terminally differentiate, transcription of a single OR dominates. Additionally, it is clear that during the window of early polygenic OR expression, total OR transcription within the cell is dwarfed by the high level transcriptional OR output observed in mature neurons. This suggests that the phenomenon of singular OR selection involves both an early, parallel vetting process among a number of co-expressed ORs, followed by a serial vetting process that accompanies the "gene-switching" phenotype[79,84] The precise role of Atf5 in either of these possible stages remains unclear; If Atf5 induction takes place during an incipient, polygenic window of OR expression, then Atf5 may be involved in the "pruning" process that eliminates all but one transcribed OR. Alternatively, if Atf5 is induced after OR transcription becomes singular, then the role of Atf5 is likely related to the stabilization of this singular choice, or to the reinforcement of all non-chosen OR alleles in a silent state. The possibility that the UPR-induced feedback may contribute to singular OR gene choice under two fundamentally distinct mechanisms prompted us to explore the exact timing of Atf5 translation in

relationship to the developmental progression of OR gene regulation in order to discern the dynamics of OR expression that provides the signal that initiates UPR in OSNs. To accomplish this, single cell RNA-seq studies from olfactory tissue can be leveraged to describe the receptor content of individual cells from a heterogeneous population, and to identify the specific cell type along developmental lines[14]. Finally, it is important to determine the direct genomic targets of Atf5 in OSNs in order to decipher the particular role Atf5 plays in stabilizing OR choice and facilitating proper OSN maturation.

Chapter 1: Identifying and Characterizing the Developmental Window in which Olfactory Neurons Translate Atf5

1.1 Identifying Cell type in which Atf5 is Translated

While Atf5 is abundantly transcribed throughout the neuronal lineage of the MOE, its translation is restricted to cells undergoing UPR. As Atf5 translation requires OR expression[84], we first wanted to distinguish between two models of UPR induction. First, that early polygenic OR expression serves as the signal that engages UPR in developing OSNs, and that the resulting Atf5 translation contributes to the elimination of all but one dominant OR. Alternatively, that singular, dominant OR expression initiates UPR, driving the feedback mechanisms that ensure stable expression of the chosen OR, and preventing the co-expression of non-chosen ORs.

We first tried to answer at what developmental stage Atf5 becomes translated in relation to other markers in the MOE by immunostaining. By co-staining using antibodies against Atf5 and markers of the HBCs, GBCs or mOSN cells (Krt5, Ascl1 and Adcy3, respectively), we find no overlap with the Atf5 positive cells (**Figure1a-c)**. While HBCs and GBCs mark cells that are enriched in basal layers of the epithelium, Atf5 antibody stains cells that reside in the middle pseudolayers. In contrast, Adcy3, a marker for mature OSNs, is detected more apically in relation to the Atf5 positive population, demonstrating Atf5 translation occurs between these developmental stages. Using a pool of OR antibodies, we see that OR protein is detected coincident with Atf5 in only a small fraction of cells, while the majority of OR positive cells are apical and thus more differentiated. This is consistent with the model that Atf5 translation is coincident with the onset of OR protein production (**Figure 1d**). From these observations, though, it remains unknown whether Atf5 translation occurs before or after either the transition to neuronal progenitors (INPs) or immature sensory neurons (iOSNs).

We generated a mouse line in which the downstream ORF of Atf5, which encodes for the functional gene product, is replaced by the coding sequence of an iRFP-P2A-iCRE reporter, what will be called the Atf5 translational reporter ("Atf5-TR") (**Figure 1f**). This allele maintains the full 5'UTR and 3'UTR, including the inhibitory upstream open reading frame. While this modified allele removes the second intron of the Atf5 gene, ATAC-seq analysis from whole olfactory epithelium reveal no signals within this region, suggesting that it does not contain any obvious regulatory element (**Data not shown**). This reagent allowed us to isolate cells that are actively engaged in the UPR, and to characterize in detail the developmental stage at which this process occurs.

To compare our Atf5-TR^{+} cells, we used fluorescent activated cell sorting (FACS) to isolate 6 distinct populations of cells from the MOE (**Fig 1e**). First, HBCs were isolated using an antibody directed against the Krt5 antigen. Second, GBCs and INP cells were isolated using Ascl1-CRE-ERt;td-tomato;Ngn-GFP mice. In this case, the coding sequence for the GBC marker, Ascl1, is replaced with a CRE-ERt cassette. Upon induction with tamoxifen, the tomato reporter becomes expressed through CRE recombination of an upstream flox-stop-flox cassette. At the same time, the Ngn-GFP allele allows for isolation of Ngn^{+} cells within the same mice. After 2 days of induction of tamoxifen, olfactory epithelium of P4-P6 mice were dissociated and sorted into either Tomato^{+}, both Tomato^{+};Ngn^{+}, or Ngn^{+} populations, allowing us to parse out three cell populations from the same pool of mice that represent the transition between the GBC and INP cell states. Third, we used the Omp-GFP^{+} mouse line to isolate cells that express the mature OSN marker, Omp. Finally, we used Atf5-TR;Omp-GFP mice to isolate Atf5-TR^{+};Omp-GFP^{-} cells, which represent cells that have initiated UPR, but that exclude mOSNs. This decision was made to obviate the possibility that the half-life of the Atf5-TR reporter protein is longer than the

endogenous Atf5 protein, owing to potential differences in the post-translational regulatory mechanisms, and that by immunofluorescence staining, endogenous Atf5 protein is drastically reduced by the mOSN stage (**Fig 1c**).

First, we sought to characterize Atf5-TR$^+$ cells transcriptionally in relation to the other major cell types of the neuronal lineage of the MOE by RNA-seq, and we visualize these results by PCA (**Fig 1g**). PCA of the sequencing libraries is useful for discerning batch effects among experiments, which is particularly important in this case where cell and library preparations were not done simultaneously. Biological replicates show tighter clustering to each other than to other isolated cell types, indicating that they represent distinct cellular populations. In addition, stem cells (HBCs) and transit-amplifying progenitors (GBCs), which are not yet committed to a neuronal cell fate, are transcriptionally more different from each other and from the post-mitotic cell types. Finally, Atf5-TR$^+$ sorted cells are transcriptionally more similar to mOSNs than the INP cells, indicating that they likely represent a transition state after cells have become dedicated neurons, and before terminal differentiation. Thus, our Atf5-TR$^+$ cells represent a distinct cellular subtype at the transcriptional level, and the developmental window of Atf5 translation is between INPs and mOSNs. Coupled with the fact that Atf5-TR$^+$ cells additionally are enriched for known markers of iOSNs (**Figure 1h**), we will hitherto consider them as such.

1.2 Transcriptional Characterization Before and After Atf5 is Translated

Pinpointing the developmental timing of Atf5-TR$^+$ cells in the MOE allows us to ask what specific genes become differentially expressed between INP and iOSN cell types. Importantly, we seek to address whether the onset of ATF5 translation coincides with developmental stages that are engaged in polygenic or largely singular OR expression. Accordingly, we did single-cell RNA-

seq on Ngn-GFP^{+} and Atf5-TR^{+} sorted cells. We used compound heterozygous mice for both the Ngn-GFP and Atf5-TR alleles. FACS was done on dissociated MOE of P10 mice to isolate Ngn-GFP^{+};Atf5-TR^{-} cells, and Ngn-GFP^{+};Atf5-TR^{+} double positive cells with the intention to clearly demarcate cells that have initiated Atf5 translation from those neuronal progenitors that have not.

We acquired single-cell RNA-seq data from 4,100 (Ngn^{+}) and 4,600 (Atf5^{+}) cells, with an average of 62,000 and 50,000 reads per cell. First, we analyzed differential gene expression between these two populations for non-OR genes. We find significantly decreased expression of known markers of the INP stage (Neurog1, Neurod1), and an increase in expression of genes known to be upregulated in immature OSNs (Gap43, Trim66) as well as mature OSNs (Omp, Gnal, Adcy3) (**Figure 2a**) in the Atf5^{+} sorted population compared to Ngn^{+}, validating the identity of these populations. That we find markers of mature OSNs enriched in the Atf5-TR^{+} cells indicate that during the process of Atf5 translation, cells may be already transitioning into the terminally differentiated state, and is also consistent with PCA analysis of our bulk RNA-seq data.

Next, we analyzed differences in OR transcript content between the two sorted populations (**Figure 2b**). As these represent cell states preceding and following the initiation of Atf5 translation, we can ask whether polygenic or singular OR expression may provide the signal to initiate UPR. For all analyses, we only count ORs as being detected if more than 1 count is uniquely mapped to it, in order to circumvent problems associated with aberrant mapping.

Our first analysis focused on identifying cells that are expressing ORs in a monogenic fashion, and at high levels. Because this condition of monogenic expression may be met by cells that are beginning to express OR transcripts at low levels, we apply a stringent cutoff where a cell will only be considered if it expresses at least 10 OR counts from a single OR gene, which would account for ~0.02% of the total transcript content of the cell on average. In total, **17.6%** and **54.6%**

of cells from the Ngn$^+$ and Atf5$^+$ populations met these requirements, respectively (**Figure 2c**). In Atf5$^+$ cells, the maximum proportion of the population expresses ~30 OR counts, with higher levels of monogenic expression being accounted for by a gradually decreasing fraction. In contrast, Most Ngn$^+$ cells express 10 OR counts (our cutoff), indicating that the monogenically expressing cells in the Ngn$^+$ population likely transition to become Atf5$^+$ as the transcriptional output of the chosen OR increases.

Second, we wanted to determine the frequency in which polygenic OR expression is observed. In this case, we do not require ORs to pass a threshold of 10 OR counts to be included in the analysis, as it is expected that early polygenic OR expression occurs at low levels. In this case, we find moderate levels of OR co-expression in both populations (**Figure 2e, f**). At the same time, we find in these cases the emergence of a dominantly expressed OR in Atf5$^+$ cells compared to the Ngn$^+$ population, further indicating that Atf5 translation coincides with singular OR selection. Finally, we find that the number of multiple ORs expressed per cell is more extensive in the Ngn$^+$ population, with up to 8 ORs detected in a single cell, although these account for very rare events.

The fact that monogenic expression commences at the developmental state that precedes Atf5 translation provides evidence that it acts as the signal that initiates UPR. At the same time, we identify more extensive polygenic OR expression in Ngn$^+$ cells well. In order to address the timing of singular OR expression further, we chose to monitor OR transcription of single cells from whole tissue, and to parse out developmental stages computationally.

From P14 mouse, we dissected and dissociated whole MOE, and did single cell RNA-seq. We sequenced 5,600 cells with an average of 55,000 reads per cell. Using Seurat single cell RNA-seq package pipeline, we performed dimensional reduction techniques, which produced a set of 21

discrete clusters of cell types (**Figure 6.1a**). Using known markers for cell types of the neuronal lineage (**Figure 6.1-6.2**), we could assign 4 major clusters into three cell types by transcriptional similarity. In total, we were able to assign 1286, 285, and 482 cells that we treated as mOSN, iOSN, and INP cell types, respectively. Using a parallel analysis as before, we found similar frequency of high level, monogenic OR expression between our sorted Ngn^+ cells and computationally identified INP cluster (**17.6%** and **20.3%)**, as well as between our sorted $Atf5^+$ cells and computationally identified iOSN cluster (**54.6%** and **58.2%**), indicating that the rate of monogenic OR expression as monitored by this approach is relatively invariant, using these two orthogonal approaches (**Figure 2d**). Interestingly, the rate of monogenic OR expression from mOSN cluster (**64.6%**) remains very similar to iOSN cluster, suggesting that by iOSN stage, and within $Atf5^+$ sorted cells, monogenic OR expression is more or less already established, and is observed as frequently as in terminally differentiated neurons. We find using two parallel approaches and a common computational pipeline, a drastic increase in the frequency of monogenic OR expression between INP to iOSN cells, consistent with its role as a developmental signal through UPR that initiates Atf5 translation. We additionally find a likewise reduction in the frequency and extent of polygenic OR transcription that coincides this this developmental transition, consistent with the idea that incipient polygenic OR expression occurs at a very early stage, and is extinguished prior to singular OR selection.

1.3 Characterizing the Nuclear Architecture of $Atf5^+$ Cells

Singular OR expression requires the pre-emptive and global repression of OR clusters, followed by de-repression of a single OR allele which physically associates with many Greek islands. Both these stages are accompanied by MOE specific changes to the nuclear

compartmentalization of OR genes and Greek islands, which can be readily detected by Hi-C[76]. Many aspects of the developmental dynamics of these processes have recently been described, but it remains unclear the nuclear architecture of cells that are actively engaged in UPR. Here, we address this by using our Atf5-TR mouse strain. Specifically, we are interested in comparing the nature of these compartments immediately before, during, and after the initiation of UPR, by Hi-C.

Accordingly, we isolated INP, iOSN and mOSN populations by FACS from two strains of mice: Ngn-GFP;Atf5-TR and Atf5-TR;Omp-GFP (Omp is a marker of mOSNs). The intention of these sorts was to isolate the earlier developmental cell type clearly from the later one in each cross, in order to avoid potential problems involving fluorophore half-life, etc. Thus, we isolated INPs, iOSNs, and mOSNs by FACS sorting Ngn-GFP^{+};Atf5-TR^{-}, Atf5-TR^{+};Omp-GFP^{-}, and Omp-GFP^{+} cells, respectively (**Figure 3a**).

Previously, Hi-C experiments have shown that OR cluster and Greek island compartmentalization is indistinguishable from non-olfactory cell types in the stem cell population, HBCs, and gradually increase as cells differentiate through the INP stage, reaching a maximum interaction frequency among either compartment in mOSNs. We thus asked whether OR cluster or Greek island hub formation is intermediate between INP and mOSNs, or whether they are indistinguishable from either cell type.

In situ HiC libraries were prepared from these FACS sorted populations, and HiC contacts were parsed into 50 KB genomic bins. Because *trans* interactions demonstrate the most dynamic changes observed between the cell types of interest, we focused our analysis on those (**Figure 3b**). Consistent with what has been published previously, we find mean interchromosomal OR cluster contacts make up ~5% of total Hi-C contacts in the genome in INP cells, reaching nearly ~10% in

mOSNs. Importantly, we also find that in Atf5-TR^{+} sorted cells, OR cluster contacts are also ~10%, indicating that by the iOSN stage of development, OR clusters have already coalesced in a way that will continue for the life of the neuron. We also see that *trans* Greek island interactions are also indistinguishable from mOSNs in cells that are translating Atf5, accounting for on average nearly 2% of all Hi-C contacts; in contrast, Greek islands contacts to other Greek islands makes up less that 1% of contacts in INP stage of development.

If singular OR selection is the signal that activates UPR and Atf5 translation, then it follows that the requirement for Greek islands to physically interact with a chosen OR allele must already be met before this developmental switch. Consistent with this, we find Greek islands have already coalesced in a way that is indistinguishable from a terminally differentiated neuron in Atf5 translation cells. We then asked whether hub formation is *dependent* on functional Atf5, which is afforded by the fact that the Atf5-TR reporter allele replaces the Atf5 coding sequence. Thus, we sorted Atf5-TR^{+} cells from Atf5-TR/TR;Omp-GFP mice, in which both copies of Atf5 are removed, but that still translates the fluorescent reporter as cells are undergoing UPR. Our results show that functioning Atf5 is dispensable for the formation of both the compartmentalization of OR clusters, as well as Greek islands (**Figure 3b-d**).

Until now, the timing of UPR engagement and Atf5 translation, and the nature of OR expression that induces this developmental switch have been imprecisely known. Using a novel Atf5 translational reporter, we find that these cells are likely iOSNs. Moreover, we show that high level singular OR transcription can be detected prior to the translation of Atf5, and that cells at this stage are forming interchromosomal contacts among OR clusters and Greek islands that are requisite for OR selection, and that persist for the life of the neuron. Moreover, the formation of these hubs occurs independently of Atf5, further confirming that it precedes this developmental

stage. These observations argue that it is singular and not polygenic OR expression that serves as the signal to transition to a functioning neuron. Still unclear is the role that Atf5 may play during this transition that leads to the stability of OR choice, and the terminal differentiation of these neurons.

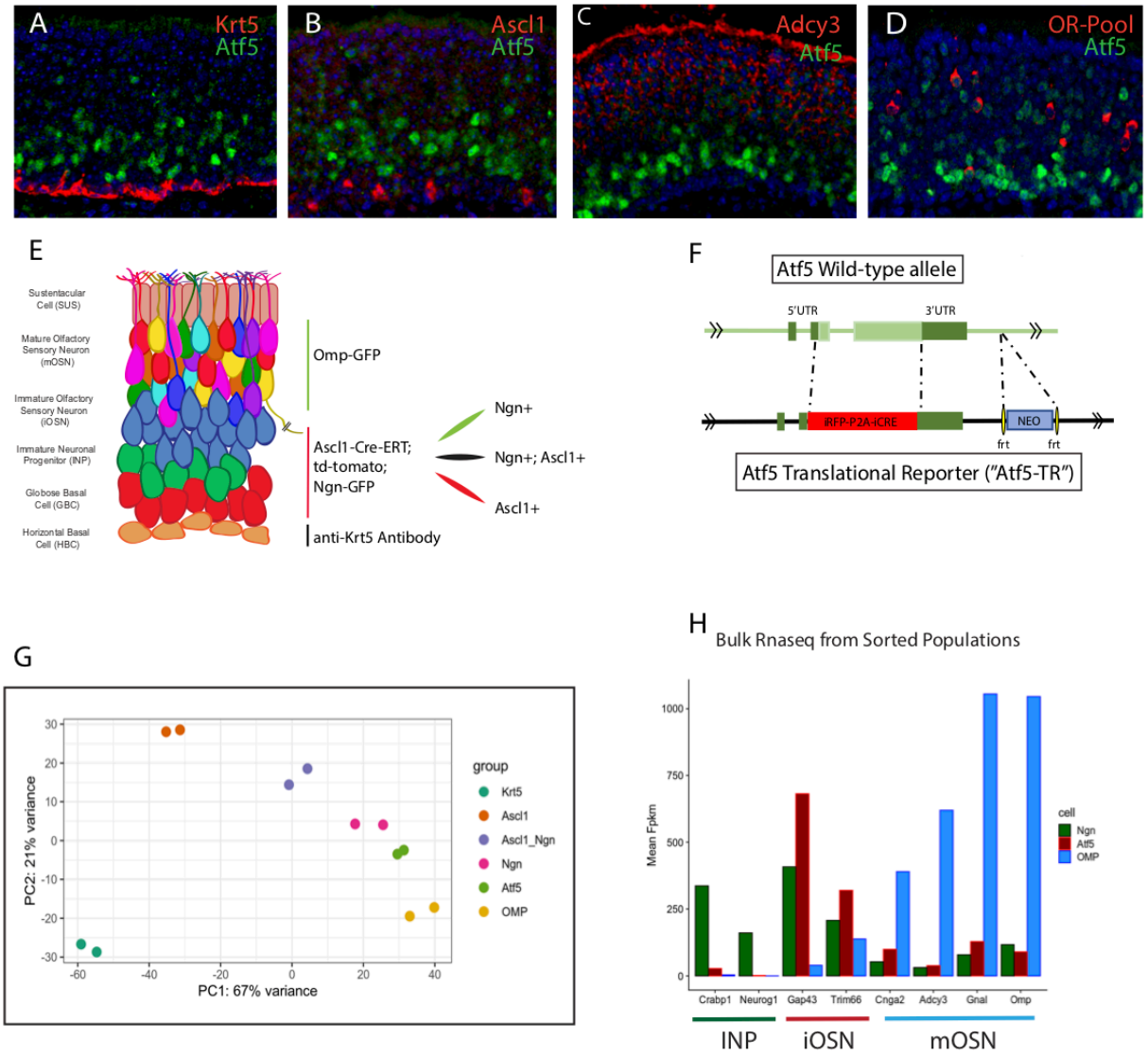

Figure 1. Bulk RNA-seq from Sorted Populations of the Neuronal lineage indicates that Atf5+ cells correspond to a developmental stage between INP and mOSN stages.

Figure 1. Atf5-TR$^+$ cells represent a transcriptionally distinct population that emerges in a developmental timeline between neuronal progenitors and mature olfactory neurons.

(A-C) Co-staining for Atf5 and markers of HBCs (Krt5), GBCs (Ascl1), and mOSNs (Adcy3). Markers for INP cells are incompatible with Atf5 staining.

(D) Co-staining for Atf5 and a pool of OR antibodies. IF was performed from MOE of 1-2 week old mice, which enriches for neuronal progenitor populations.

(E) Schematic of the developmental cell types of the MOE that give rise to olfactory neurons. In addition to the Atf5-TR$^+$ sorted populations, 5 other cell types were sorted using antibodies or genetically encoded reporters to isolate HBCs (Krt5$^+$), GBCs (Ascl1-Cre-ERT;td-tomato$^+$), GBCs transitioning to INP cells (Ascl1-Cre-ERT;td-tomato$^+$;Ngn-GFP$^+$), INPs (Ngn-GFP$^+$), and mOSNs (Omp-GFP$^+$).

(F) Atf5 Translational Reporter allele (Atf5-TR) replaces the coding sequence of the functional Atf5 gene with an iRFP-P2A-iCRE reporter.

(G) PCA analysis of RNA-seq libraries prepared from 6 sorted populations of the MOE.

(H) Mean FPKM values among replicates from RNA-seq from three sorted populations for genes representing three developmental timepoints.

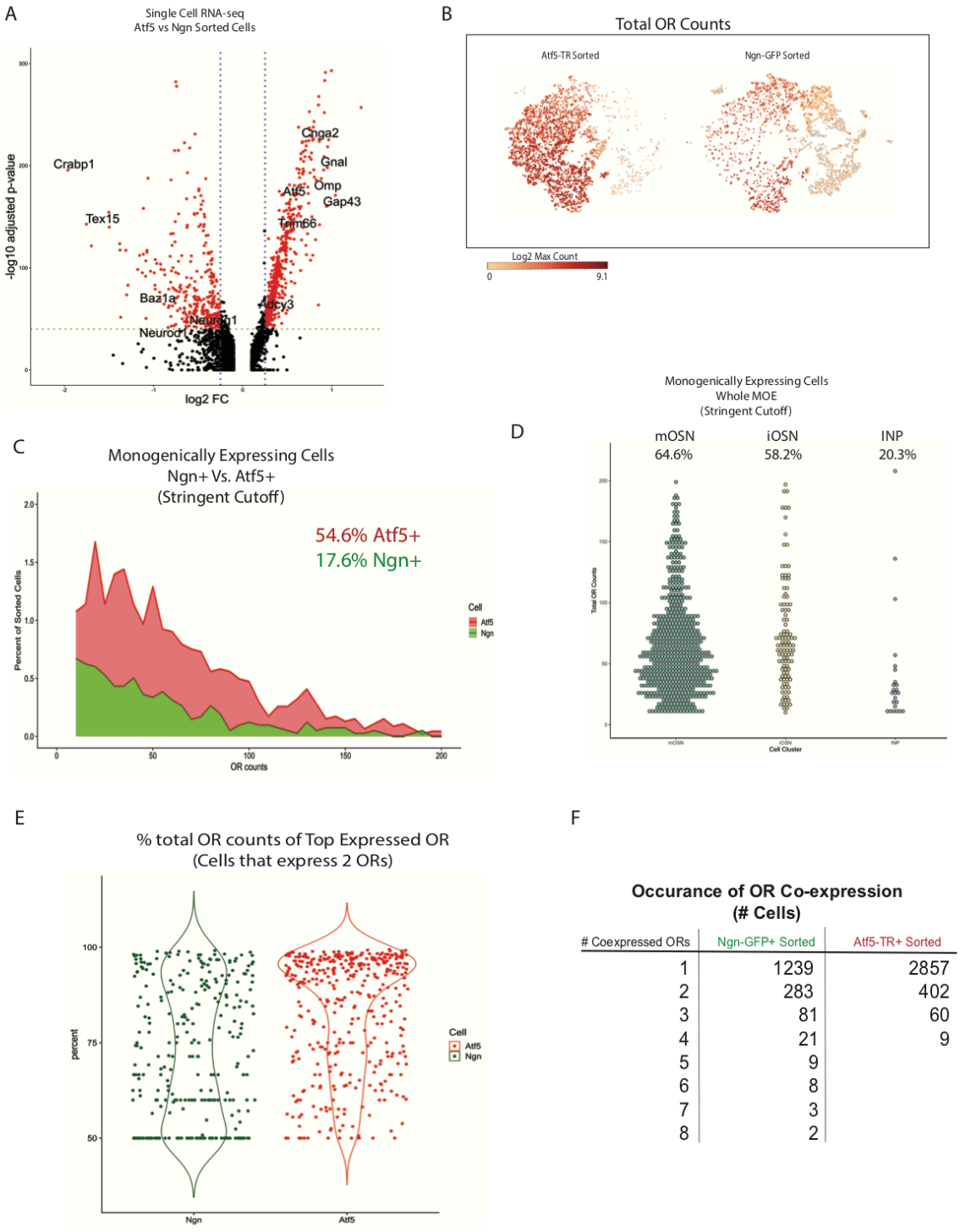

# Coexpressed ORs	Ngn-GFP+ Sorted	Atf5-TR+ Sorted
1	1239	2857
2	283	402
3	81	60
4	21	9
5	9	
6	8	
7	3	
8	2	

Figure 2. Single Cell Rnaseq from NGN+ and Atf5+ sorted populations.

Figure 2. Single Cell RNA-seq from Ngn-GFP$^+$ and Atf5-TR$^+$ sorted populations, and MOE demonstrate singular OR expression precedes Atf5 translation.

(A) Volcano plot of differentially expressed genes between the two populations of cells. Using cutoffs of –log10(adjusted-Pvalue) > 30 and log2 fold change in expression greater than 20% as averaged across all sorted cells, we identify 238 and 430 genes that are down and upregulated, respectively, between Atf5-TR$^+$ and Ngn-GFP$^+$ populations. These genes include known markers for neuronal progenitors, as well as markers for iOSNs and mOSNs.

(B) Ngn$^+$ and Atf5$^+$ sorted populations that monogenically express OR at high levels represent 17.6% and 54.6% of cells, respectively. All ORs require at least 1 count to be included in the Analysis, and the "stringent cutoff" requires that the monogenically expressed OR have at least 10 counts.

(C) Occurrence of Co-expression from Ngn$^+$ and Atf5$^+$ sorted cells. A "relaxed" cutoff is used, which only requires more than 1 count for an OR to be counted as expressed.

(D) Single Cell RNA-Seq from whole OE, showing the cells that express OR monogenically from three clusters of cell populations. The "stringent" cutoff of required OR counts is used.

(E) Comparison of the percent of cells from either sorted populations, or the clusters identified, that exhibit polygenic (expressing >1) OR expression using the "relaxed" cutoff

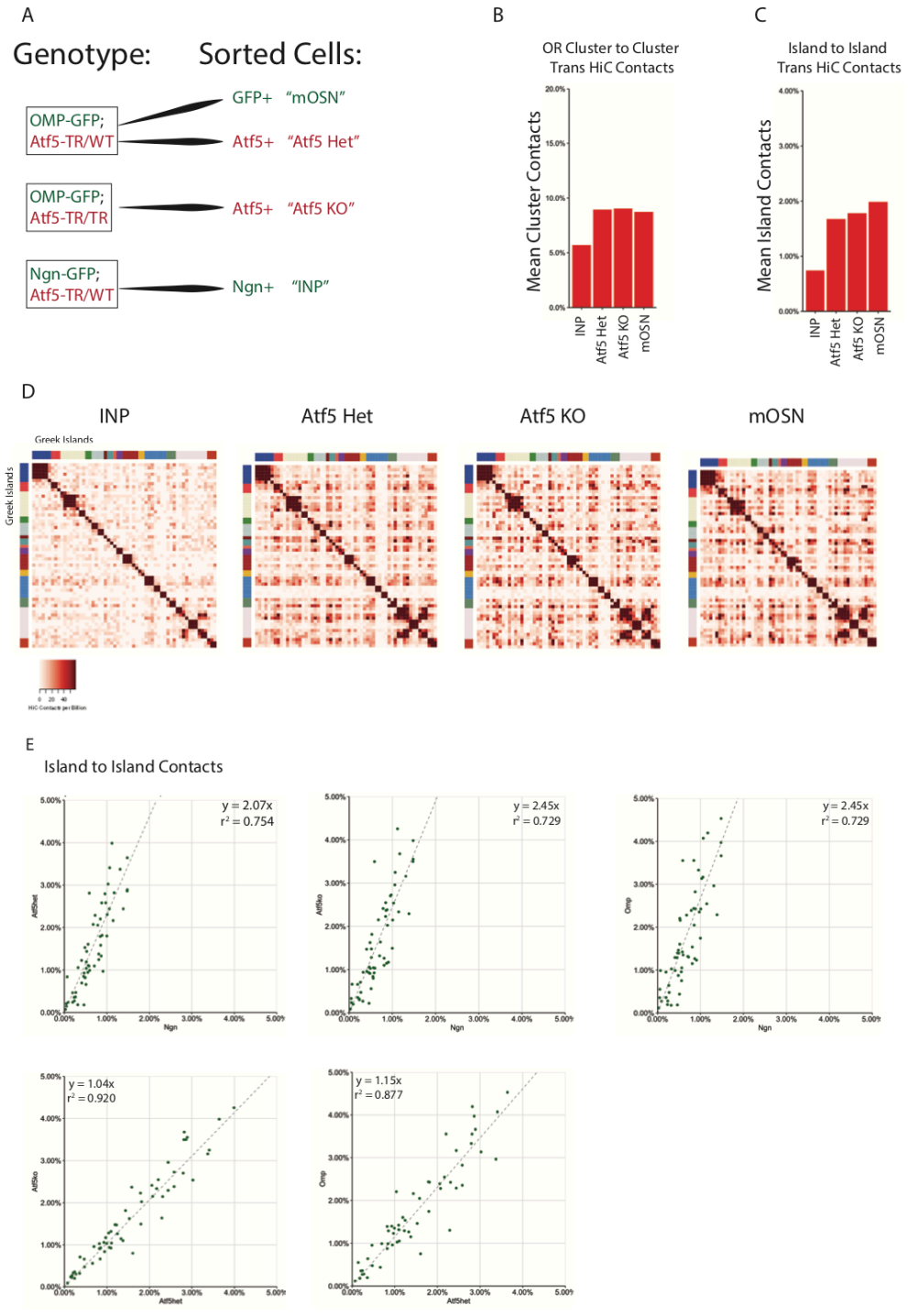

Figure 3. Interchromosomal contacts are formed in Atf5+ expressing cells, and is Atf5 independent

Figure 3. Interchromosomal Contacts are formed in Atf5^{+} expressing cells, and are Atf5-Independent

(A) Schematic showing the design of the experiment to isolate 4 cell populations using 3 mouse crosses. For segregating cell populations pooled from the same mice, the earlier developmental cell type was isolated from the later one. I.e., in the OMP-GFP;Atf5-TR/WT cross, Atf5^{+} cells were GFP-, and for the INP sorted population, Ngn-GFP^{+} cells were Atf5-TR-.

(B) Mean cluster contacts among OR clusters as assessed by in situ Hi-C, comparing the 4 sorted populations of cells. Only interchromosomal contacts are considered.

(C) Mean cluster contacts among Greek islands among the 4 sorted populations.

(D) Heatmap showing pairwise comparisons of HiC contacts between Greek islands, ordered by chromosome. Cis contacts account for a high portion of HiC contacts, and are already formed by the INP stage. In contrast trans contacts emerge by the Atf5^{+} cell stage, and are stable through development. While this is a developmentally regulated process, it does not depend on Atf5.

(E) Scatterplots showing changes in trans Greek island contacts, as shown as the fraction of total HiC contacts. In contrast to the comparison between INP cells and all other cell types examined, which show an global increase in trans contacts among Greek Islands, there is no substantial change between Atf5 Het and Atf5 KO cells, or between Atf5 Het and mOSN cells.

Chapter 2: Characterizing a Role for Atf5 in Proper Neuronal Function

2.1 Identifying Atf5 Dependent Genes in the MOE

In order to identify the role of Atf5 in developing neurons, we performed chromatin-immunoprecipitation followed by next generation sequencing (ChIp-seq) to identify the targets of this transcription factor from the whole MOE. We find ~600 peaks that are significantly enriched in two biological replicates (**Figure 4a**). As evidence against a direct role in regulating either Greek islands or OR genes, there is no significant signal for Atf5 binding within these genomic regions (**Figure 4a, data not shown**). Instead, Atf5 is expected to act indirectly to stabilize OR expression through its target genes.

The most significantly enriched motif identified among Atf5 bound regions reveals a CRE/CAAT binding site motif (**Figure 4b**), common among the family of bZIP transcription factors to which Atf5 belongs, and similar to a binding site identified using vitro approaches[90,91]. The two half sites suggest the Atf5 may heterodimerize with a yet unknown binding partner.

By assigning Atf5 binding sites to its nearest gene, we can begin to unravel the role that Atf5 may play mechanistically. Atf5 binds to mostly intergenic (32.4%) and intronic regions of the genome (46.0%); only a fraction of sites occupies promoters of genes (17.0%) (**Figure 4c, e)**. This is perhaps surprising given the expectation that Atf5, as a stress response transcription factor, would be geared toward the immediate resolution of the stress response. By targeting the promoter regions of its target genes, Atf5 would swiftly be able to recruit transcriptional machinery to these sites. Instead, the genomic distribution of Atf5 targets may point to an atypical role this transcription factor plays in regulating the transcriptome during UPR. Therefore, for further

analysis, Atf5 target genes were not filtered based on a maximum genomic distance to the binding site. Consistent with a role in resolving the UPR, genome ontology analysis revealed that these 600 Atf5 binding sites are enriched for genes that become activated in conditions to ER stress, in response to unfolded proteins, and include many of the tRNA synthetase genes (**Figure 4d)**. Additionally, some GO terms indicate that Atf5 binds genes that may be involved in a range of downstream regulatory processes, including chromatin modification, translational initiation, and mRNA splicing.

Next, we sought to determine which Atf5-bound genes become dysregulated when Atf5 is genetically ablated. Atf5 KO mice demonstrate a partially penetrant neonatal lethality phenotype, presumably owning to a suckling deficit secondary to an olfactory defect[85]. In adult Atf5 KO mice, there is a striking developmental defect leading to arrest prior to the fully mature OSN stage, which leads to ~1000 fold decrease in the number of mOSNs detectable by IF (**Figure 5a,b**)[84]. RNA-seq of whole MOE from Atf5 WT and KO mice reveals a large number of genes that become dysregulated in the absence of Atf5 (**Figure 5c).** Markers for developmentally regulated genes that define iOSN and mOSN lineages are markedly reduced, while markers for earlier progenitor lineages are slightly increased (**Figure 5e**), suggesting an expansion of these cell types as an accompanying effect of the loss of more mature cell types. As previously reported, there is a severe reduction in OR transcription (**Figure 5d**), at least in part as a consequence of the instability of singular OR expression.

Genes that are bound by Atf5 are predominantly downregulated in the Atf5 KO, suggesting that Atf5 acts as a transcriptional activator (**Figure 5f**). This set of ~220 genes therefore comprise direct targets of Atf5 that are dependent on Atf5 for transcriptional activation, what will be referred to as the "Atf5 dependent genes". Importantly, by looking at transcript levels of Atf5 dependent

genes from sorted populations (**Figure 1g, Figure 5g**) we observe that many of these genes are upregulated in the mature OSN stage. This was a surprising result, given the observation that Atf5 protein is downregulated in mature neurons.

Among our 200 Atf5 dependent genes, we can initially and broadly parse genes into categories we predict to be the effectors of proper neuronal function, and the targets that underlie the critical role of Atf5 in the olfactory system (**Figure 5h**). Not surprisingly, we find genes involved in ER and Golgi homeostasis (Herpud1, Tmbim6, Manea, Calm1, Gfy). We also find genes involved in the proper processing and function of OR proteins including chaperone proteins (Rtp1, Rtp2, Ric8b), and signaling molecules (Gnal, Gnb1). Additionally, we've identified a collection of genes involved in axon transport, axonogenesis and cell adhesion (Plxna1, Map1b, Cntn4, Ncam1), indicating a potential Atf5-specific role in OSN targeting to the OB, which may coordinate with OR protein in proper glomerular targeting. Finally, we find a number of transcription factors and chromatin modifying enzymes (Cbx4, Trim66) which likely enforce downstream effects involved on the stabilization of OR choice and proper OSN maturation. Collectively, these findings motivate exciting starting points for further inquiry regarding the mechanisms and actors involved in proper neuronal differentiation and function.

Nascent OR translation, through mechanisms that are still unclear, are recognized as unfolded proteins in the ER. In Atf5 KO mice, OR proteins can be detected as punctate aggregates localized in the ER, indicating that Atf5 plays a role in facilitating normal OR movement through this protein processing organelle[84]. We find Atf5 dependent genes include chaperone proteins with known roles in OR trafficking and signaling, including Rtp1, Rtp2, Gnal and Ric8b[88,9293]. Identification of putative OR chaperones have been motivated by the fact the OR expression in heterologous systems is notoriously difficult, hindering OR-ligand studies and in vivo OR protein

production. This is presumably because OR specific chaperone proteins are also OSN specific. Two Atf5 dependent genes, Rtp1 and Rtp2, for example, are transmembrane proteins that are highly and specifically expressed in the MOE[88]. In HEK293T cells, they have been shown to coprecipitate with, and enhance the surface expression of OR proteins. Additionally, Gnal encodes for the olfactory specific G-alpha subunit[31]. Ric8b is specifically expressed in olfactory neurons, and has been shown to promote cell surface expression of ORs in a heterologous system, as well as promote their functional expression, by assisting in the coupling of OR proteins to G(olf) alpha[92]. Knock out models for these individual chaperone proteins have shown dysregulation in OR transcription, and maturation defects, similar to what we observe in Atf5 KO mice[94,95]. Thus, at least one role for Atf5 in the proper function of olfactory neurons is to coordinate the transcriptional activation of a set of chaperone proteins that promote the productive expression of OR proteins to exit the ER and successfully traffic to the cell membrane, as well as support OR signaling function. Considering that nascent OR translation is likely the signal that engages the unfolded protein response, this regulatory module that facilitates proper OR expression would also elicit the resolution of the UPR, and would explain why Atf5 is transiently translated.

2.2 Characterizing Cell Type Specific Gene Dysregulation in the Atf5 KO

Atf5's role in the olfactory system may be multi-modal; it may coordinate the activation of sets of genes that address different aspects of proper neuronal function, which collectively result in a fully functional mature OSN that has properly targeted the appropriate glomerulus in the bulb, and will stably express a single OR for the life of the neuron. Moreover, a model of multimodal Atf5 function may be temporally regulated, such that stable OR expression precedes productive OR trafficking, which precedes proper axon targeting, for example. To address the dynamics of

transcriptional dysregulation of Atf5 dependent genes in different developmental cell types, we performed single cell RNA-seq from WT and Atf5 KO whole MOE from P14 mice, an age at which the diversity of neuronal subtypes is greatest.

After filtering and scaling the data, sequencing libraries from the two genotypes were integrated using Seurat single cell RNA-seq package pipeline. Dimensional reduction techniques produced a set of 21 discrete clusters of cell types shared between the two genotypes (**Figure 6.1a**). Using known markers for the major, molecularly defined cell types of the MOE, we parsed the clusters into non-neuronal cell types, microvillous (MV), and sustentacular (SUS), as well as the neuronal lineage, HBCs, GBCs, INPs, iOSNs, and mOSNs (**Figure 6.1-6.2**). Genes that define the INP lineage were distributed across two clusters, so we subsequently called these cell types INP1 and INP2. This is consistent with a previous single cell RNA-seq study that found that the INP stage is heterogeneous and can be parsed into different groups based on differential expression of key transcription factors and cell cycle genes[14].

Differential gene analysis for the 6 cell types that give rise to OSNs between the two genotypes reveal transcriptional differences neither in stem cells (HBCs), where Atf5 is not transcribed, nor in early neuronal progenitors (GBCs, INP1), where Atf5 is not translated. Instead, we find that transcriptional dysregulation commences during the INP2 stages (**Figure 7**). This is also consistent with observations from our single cell RNA-seq data from NGN-GFP$^+$ and Atf5-TR$^+$ sorted populations which demonstrate that infrequent high level OR expression is observed in Ngn-GFP$^+$ cells (**Figure 2c**). Likely the cell type defined as the INP2 cluster in these data includes cells that are initiating Atf5 translation, and account for the early dysregulation of genes that are both direct and indirect targets of Atf5. The extent of gene dysregulation reaches its peak in the iOSN cell type, reflecting the state of developmental arrest that predominates in the Atf5

KO MOE. The verity of the clustering agrees with bulk sequencing and IF experiments in Atf5 KO (**Figure 5b,e**). Additionally, cells in clusters that belong to the mOSN lineage account for 26.9% of all cells sequenced in the WT MOE, and only 4.5% of total cells in the KO. In contrast, the cells that are in the iOSN stage present comparable numbers, making up 5.4% and 7.6% of total cells sequenced in the WT and KO MOE, respectively.

Interestingly, the Atf5 dependent genes that appear as most significantly down regulated in the Atf5 KO in the INP2 stage include a handful of chromatin modifying enzymes, Cbx4 and Trim66,which have been associated with transcriptional repression[96,97,98]. It is in fact in the later iOSN stage that the most significant transcriptional effects on OR associated chaperone proteins can be discerned. This may suggest that one of the earliest events that accompanies Atf5 translation involve epigenetic changes that lead to gene silencing, followed by the activation of genes that act to faithfully traffic a suitable OR protein to the cell surface.

Here, we identify the first known genome-wide targets of the stress-response transcription factor, Atf5 in olfactory neurons. Coupling this ChIp-seq and our RNA-seq data from Atf5 KO MOE, we identify a set of ~200 Atf5 dependent genes, which include a handful with known functions in facilitating proper OR expression, axon development, ER homeostasis, as well as chromatin modifying enzymes and transcription factors. By single-cell RNA-seq, we pinpoint the developmental stages in which these genes become dysregulated. We find the earliest transcriptional dysregulation occurs during INP stage of development, consistent with previous results that this is the developmental window in which Greek island compartmentalization and singular OR transcription initiates, transmitting the signal that leads to Atf5 translation.

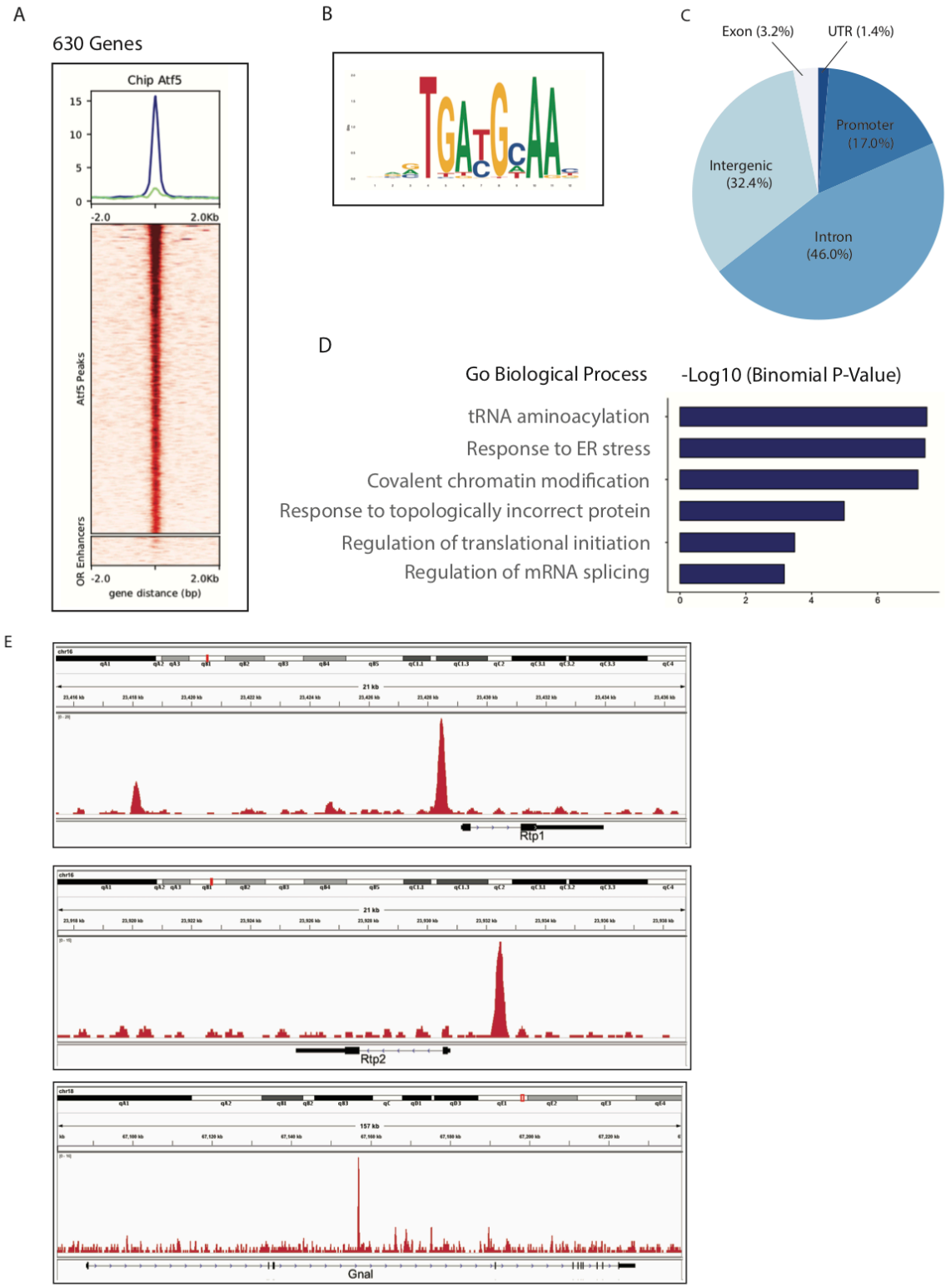

Figure 4. Chip-seq for Atf5 idendtifies ~600 bound loci.

Figure 4. ChIp-seq for Atf5 identifies ~600 bound loci.

(A) Atf5 ChIp-seq plotted across either 600 loci considered significant by using HOMER between two biological replicates (top), or the ~60 identified Greek Islands (bottom). Mean signal across all loci are summarized above the plot for each genomic class.

(B) De Novo Motif analysis using HOMER identifies a CRE/CAAT site

(C) Percentages of Atf5-bound loci that are categorizes as either intergenic, intronic, promoter regions, exons or UTRs.

(D) Gene Ontology term from the Biological Pathway analysis using GREAT

(E) Gene track showing ChIp-seq signal for Atf5 at three bound loci. (Top) RTP1 is bound at the promoter, and at a position 10 Kb upstream from the TSS. (Middle) Rtp2 is bound in the promoter region. (Bottom) Gnal (Olfactory specific Galpha subunit) is bound intronically.

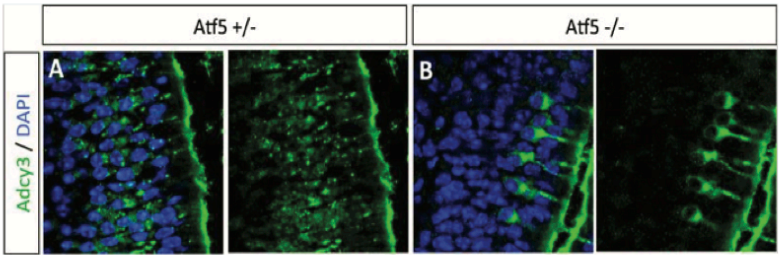

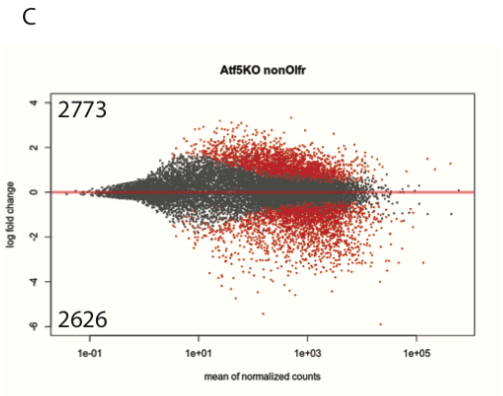

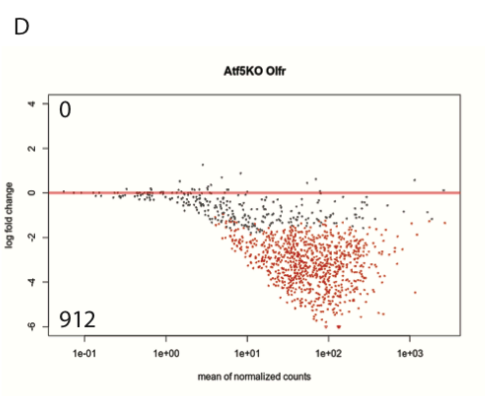

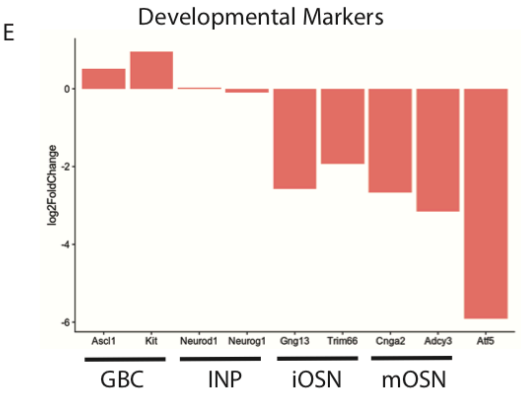

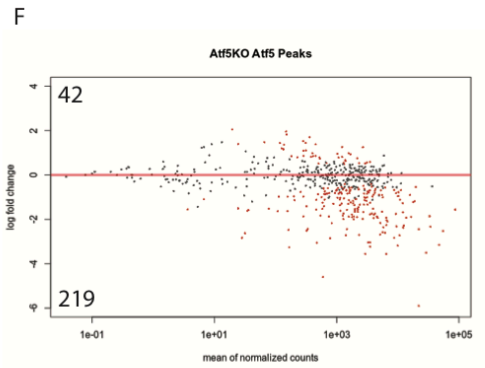

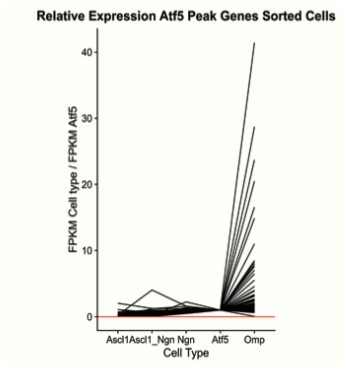

H

Category	Genes
ER Stress Response	Herpud1, Tmbim6
Chaperone, Coreceptor	Rtp1, Rtp2, Ric8B, Gnal, Gnb1
Transcription Factor	Mef2b, Creb3l1, Uncx, Klf7 Rfx3, Tshz2
Chromatin Modifier	Brdt, Hdac9, Cbx4, Trim66
Axon transport/guidance, Cell adhesion	Plxna1, Kif1a, Map1b, Dcdc2a Cntn4,Ncam1

Figure 5. RNA-seq from whole MOE identifies Atf5-bound genes that become dysregulated in Atf5 KO

Figure 5. RNA-seq from whole MOE identifies Atf5-bound genes that become dysregulated in Atf5 KO

(A,B) Immunofluorescence in control (A) and Atf5 KO (B) MOE using mature OSN marker Adcy3.

(C) MA plots from RNA-seq comparing WT and Atf5 KO mOSNs of all non-OR genes. Red dots represent genes that are significantly differentially expressed (FDR < 0.025) between samples; 2773 genes are upregulated in Atf5 KO, and 2626 genes are downregulated.

(D) MA plots sub setting for only ORs. 912 ORs are significantly downregulated in the KO and 0 are upregulated.

(E) Log2 Fold Change values of developmental markers from 5 stages of development.

(F) Among ~600 Atf5 bound genes, ~200 are downregulated and 40 are upregulated

(G) FPKM values of bulk RNA-seq from developmentally sorted cell types of the MOE. Y-axis is the ratio of FPKM values between the presented cell type and $Atf5^{+}$ sorted population.

(H) Handful of Atf5-dependent genes, some with known roles in proper OSN function.

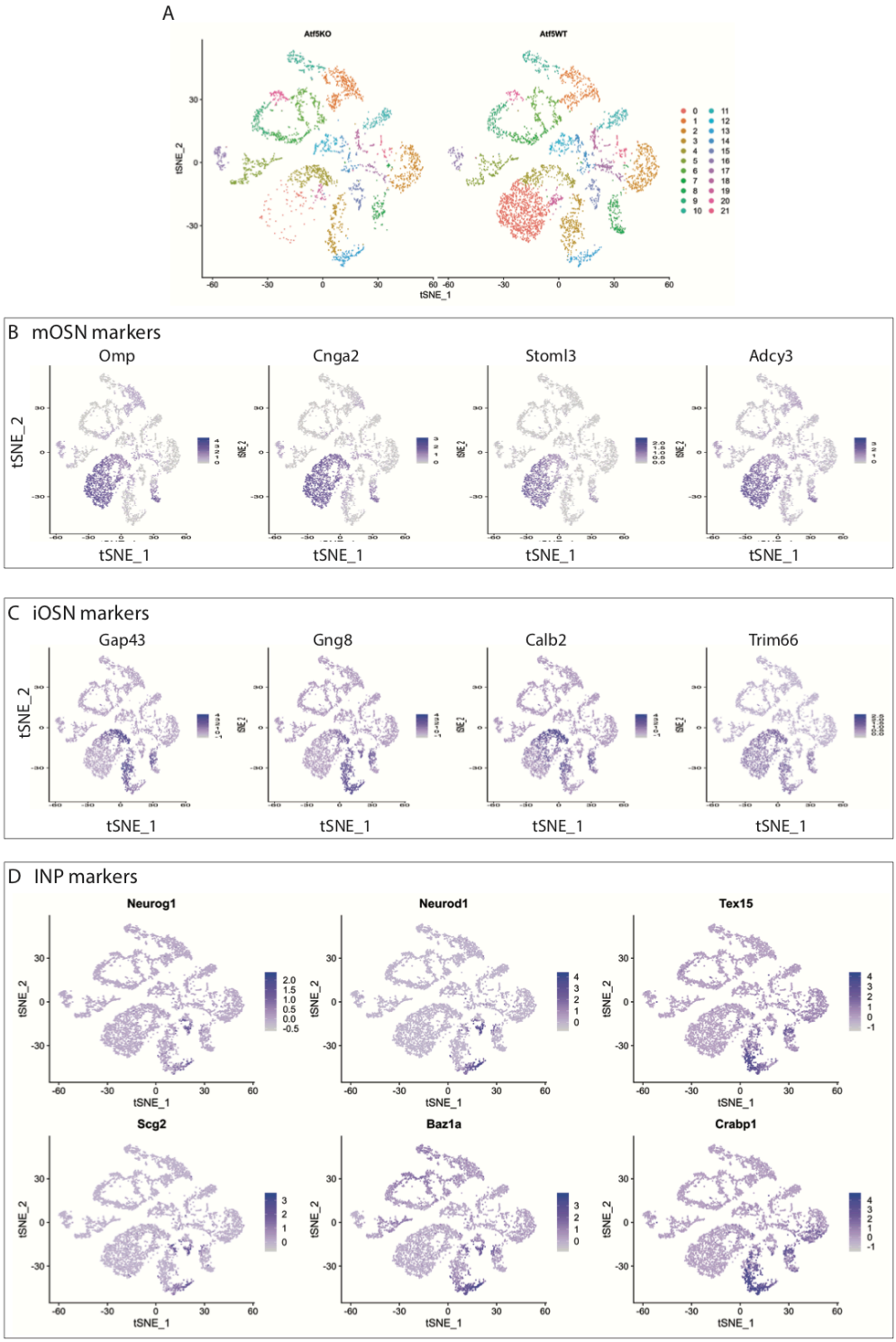

Figure 6.1 Expression of known markers of cell identity in the olfactory epithelium

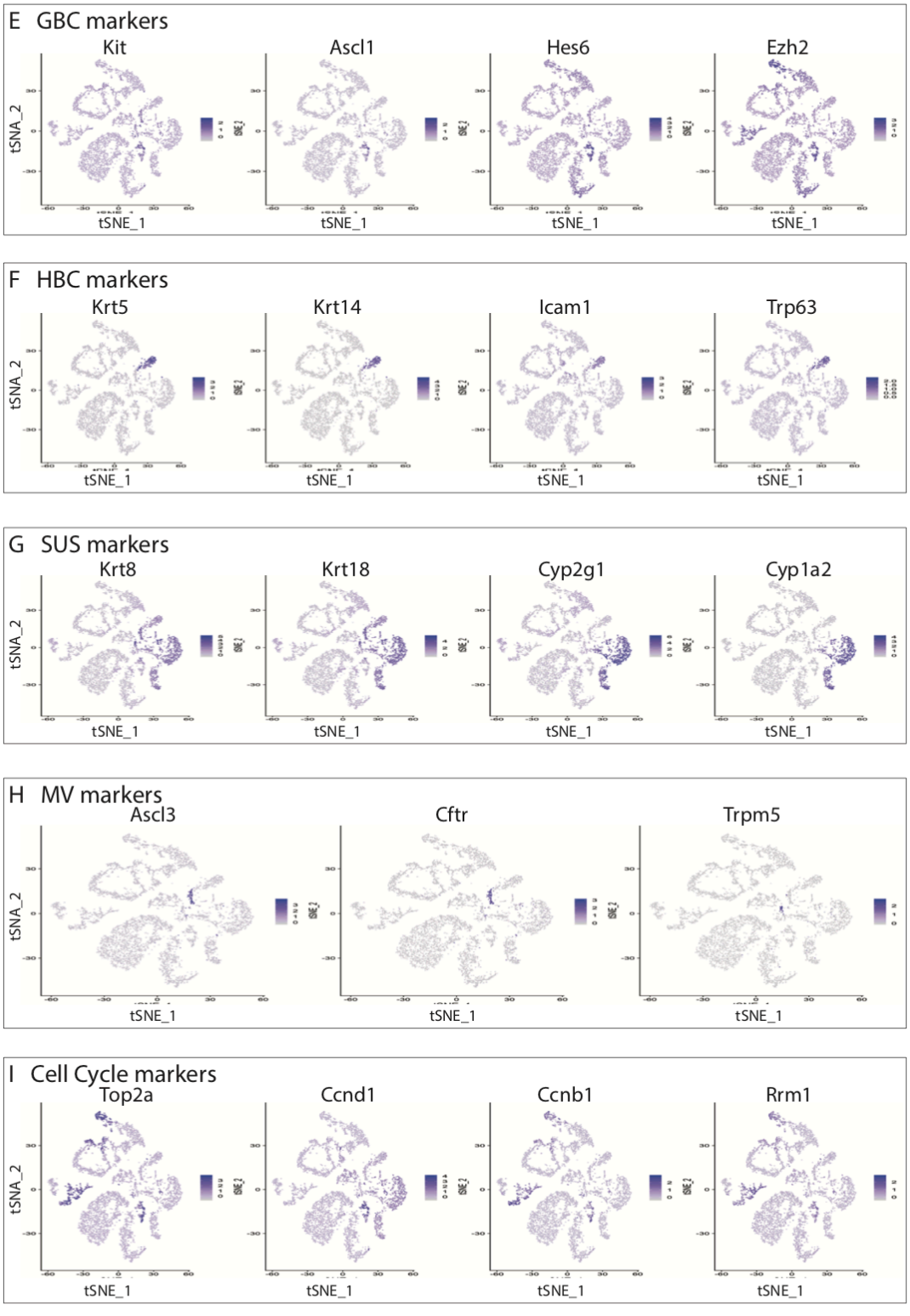

Figure 6.2 Expression of known markers of cell identity, and cell cycle in the olfactory epithelium

Figure 6.1, 6.2 Expression of known markers of cell identity in the olfactory epithelium

(A) Dimensional reduction of the Atf5 KO and Atf5 WT single cell RNA-seq data sets, visualized by tSNE. Clusters of interest were assigned cell type identities using known molecular markers of developmental stages of interest **(B-I)**

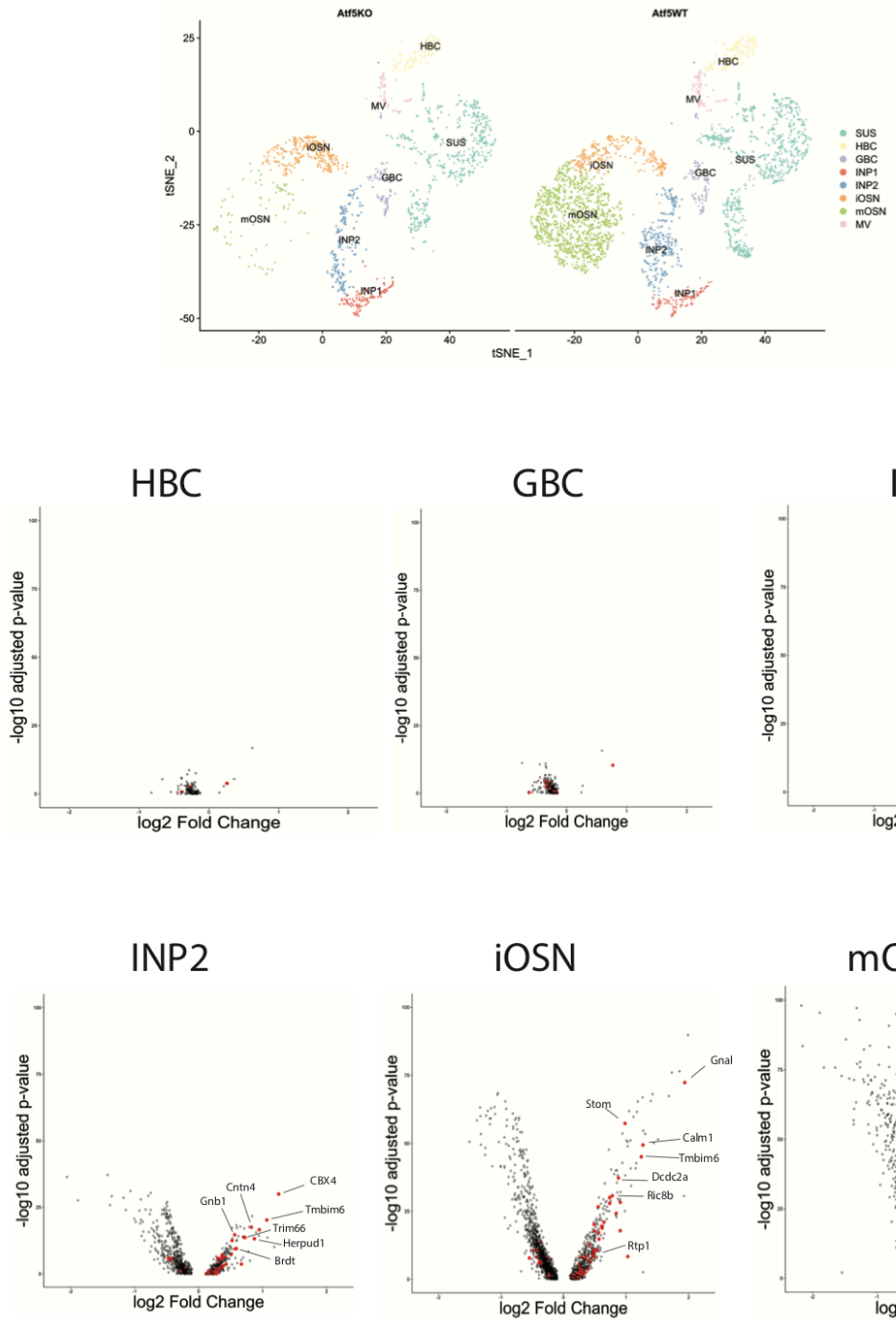

Figure 7. Differentially expressed Atf5 dependent genes (red) between Atf5 KO and WT MOE, comparing cells clustered as putative cell types

Figure 7. Differentially expressed genes between Atf5 KO and WT MOE by single cell RNA-seq

(A) The cell clusters identified in figure 6, showing only cells that descend from the resident olfactory stem cells.

(B) Volcano plots of appropriate cell clusters comparing the two genotypes. Genes in red show Atf5 dependent genes. Differentially expressed genes were identified using Wilcox rank sum test, and filtered for genes with a log2 fold change expression > 0.1 of the average of all cells used in the comparison.

Chapter 3: Atf5 is a Stress-Response Transcription Factor that Plays a Unique Role in the Olfactory System

3.1 Atf4 Cannot Replace Atf5 Function

The realization that Atf5 directly regulates gene expression programs that do not fall within the "traditional" responders of the UPR pathway raises the question of what molecular mechanisms altered and expanded the repertoire of biological responses to ER stress. This question is particularly pertinent, considering the fact that an important paralogue of Atf5, namely Atf4, is also expressed in the olfactory epithelium. Atf4 is a ubiquitously expressed stress response transcription factor, that, like Atf5, is the target of a number of transcriptional programs that become active in the presence of a variety of cellular stresses, including ER stress, oxidative stress and amino acid deprivation[99,100]. Atf4 also harbors a cryptic upstream open reading frame that leads to preferential translation in conditions of limiting initiator methionine, a consequence of eif2a phosphorylation[86]. Atf4 targets a number of genes which collectively serve to resolve the source of stress by increasing protein processing machinery in the cell. Atf4 also belongs to the bZIP family of transcription factors and is known to homodimerize as well as heterodimerize with other transcription factors to direct transcriptional activation of target genes[101,102].

Despite parallel roles in sensing ER stress between Atf4 and Atf5, the stark phenotype in the Atf5 KO raises the possibility that Atf5 may possess unique properties that are exploited in the olfactory system, but that cannot be sub-served by Atf4. Importantly, Atf4 KO models do not exhibit an olfactory phenotype (**Data not shown**).

Atf4 transcription is less dynamic but more expansive than Atf5. RNA-seq from sorted populations representing distinct developmental stages reveals that while Atf4 transcription is relatively constant among the different cell types observed, Atf5 transcription dramatically

increases from the GBC stage up to the Atf5^{+} cells (**Figure 8a**). Importantly, Atf5 transcription remains high in the mOSN stage of development, though protein translation is terminated (**Figure 8a, 1c)**. From single-cell RNA-seq data, we see that Atf5 transcription is restricted to cells of the neuronal lineage, while Atf4 can be detected in non-neuronal cell types as well (**Figure 8b**). The specificity and high level of transcription of Atf5 suggest that Atf5 may play a special role in the olfactory system that, in addition to promoting proper OR protein production, may be critical for proper neuronal development.

A possible candidate for the cooption of the UPR to neuronal processes could be the preferential transcription of Atf5 in iOSNs, instead of the canonical UPR effector Atf4. Atf4 transcription in the MOE comparably lower than Atf5, and Atf4 ChIP-seq in wild type MOEs does not return any peaks (**Figure 9a, 8i**), preventing us from answering whether the two factors are redundant. Therefore, to explore the functional redundancy between Atf4 and Atf5 in the MOE, we generated a new mouse strain in which we replaced the coding sequence (CDS) of Atf5 with the Atf4 CDS (Fig), via homologous recombination, seeking to elevate the expression of Atf4 protein at the levels of Atf5 (**Figure 8c**). Here, as is the case with our Atf5 translational reporter, the Atf5 coding sequence is replaced with Atf4, removing the second intron, but maintaining the endogenous Atf5 5'UTR, including the cryptic upstream open reading frame. This, Atf4 will be transcribed from the Atf5 locus, and will preserve upstream regulatory sequences that normally allows for regulated translation of Atf5 during UPR.

Quantification of RNA levels in this mutant confirms that Atf4 transcript levels are raised to the level that Atf5 is normally (**Figure** 8i). Immunostaining for Atf4 in WT MOE show infrequent and sporadic translation of Atf4 in the WT mouse. In contrast, Atf5 Swap mouse shows much higher levels of Atf4 protein (**Figure 9d**). Interestingly, Atf4 protein in the Atf5 Swap mouse

occupies the nuclei of cells that reside in the more apical regions of the MOE (**Figure 8e**). This is in contrast to endogenous Atf5 staining in WT mice, which is present in the more basal layers of the MOE (**Figure 1a-d**). Staining for a markers of mature neurons (Adcy3 and Calmegin) show a drastic reduction in the number of cells that reach this developmental stage, similar to what is observed in the Atf5 KO mouse (**Figure 8d, 5a,b**). This indicates that Atf4 transcription in place of Atf5, while leading to more Atf4 protein, cannot replace the function of Atf5, and demonstrates the same developmental defect as seen in Atf5 KO MOE. As Atf4 translation is a sensor of UPR, the observation that Atf4 protein persists in the apical layers of MOE may indicate that in the Atf5 swap, UPR is not properly resolved.

RNA-seq from Atf5 Swap MOE shows a large number of genes that become significantly differentially expressed compared to WT (**Figure 8f)**. Like in the Atf5 KO, OR transcription is predominantly decreased (**Figure 8g**). Additionally, we notice downregulation of important developmental markers that is established by the iOSN cell stage (**Figure 8h**), providing further evidence that the Atf5 Swap mouse exhibits a developmental defect similar to what is observed in Atf5 KO.

We next asked whether the transcriptional deficit in the Atf5 Swap is due to dysregulation of Atf5 dependent genes. Indeed, ~120 Atf5 peak genes are downregulated in the Atf5 Swap (compared to ~220 genes in the Atf5 KO), using FDR < 0.025 as statistically significant (**Figure 9d**). This result suggested the possibility that Atf4 may bind to and transcriptionally activate a subset of Atf5 peaks. To address this, we performed ChIp-seq using an antibody directed against Atf4 in Atf5 Swap and control MOE (**Figure 9a**). From our Chip-seq results, we found 172 Atf4 peaks, compared to ~600 Atf5 consensus peak set, among which 135 binding sites occupy the same genomic regions (**Figure 9b**). Visualizing the ChIp-seq signal on these genomic regions, we

can compare binding affinity for Atf4 and Atf5 to these locations between the genotypes used in this experiment (**Figure 9a**). Consistent with our immunofluorescence results using Atf4 antibody, we find that there is greater Atf4 binding signal in the Atf5 Swap, although there is low level signal in the WT MOE. Importantly, Atf5 ChIp signal is abolished in the Atf5 Swap, providing evidence that our At5 antibody is not cross-reacting with other proteins. The top motif identified from Atf4 binding sites produces a motif logo very similar to the top motif from Atf5 binding sites (**Figure 9c, 4b**).

We have generated a genetic tool to ask whether ectopic Atf4 expression could perhaps rescue the olfactory phenotype we observe in the Atf5 KO MOE, by knocking in the Atf4 coding sequence in place of Atf5. This Atf4 Swap allele maintains endogenous regulatory elements and the 5'UTR that control Atf5 transcription and translation, respectively. We find that this model produces more Atf4 protein, and we can subsequently detect increased genomic occupancy of this transcription factor by ChIp-seq. Importantly, Atf4 binds only a fraction of Atf5 binding sites. At the same time, we observe drastic reduction in OR transcription, and a developmental defect that seems to commence at the iOSN stage, and culminates in a severe reduction in mature olfactory neurons. Thus, Atf4 is directed to a subset of Atf5 binding sites, but cannot replace the function of Atf5.

3.2 Identifying Atf5 Cofactors Important for Normal Olfactory Function

The finding that Atf4 over expression cannot replace the function of Atf5 indicates that Atf5 plays a special role in the proper development of MOE, and for proper OR expression. Indeed, only a portion of the targets of Atf5 are similarly bound by Atf4 in the Atf5 Swap mouse, despite

increased Atf4 protein. This may indicate that Atf5 targets a subset of olfactory specific sites by binding to a set of yet unknown protein partners.

The top motifs identified for both Atf4 and Atf5 ChIp-seq experiments suggest strikingly similar binding preferences for these transcription factors (**Figure 9c, 4b**), and both look like CRE/CAAT binding sites. CRE/CAAT sites are found in number of genes with roles in modulating the stress response, and are bound by a diverse array of DNA-binding proteins[103]. Atf4 and Atf5 and known to bind to such sites, and are known to complex with a variety of cofactors to accomplish this[102], including the Cebp family of transcription factors. Here, we took a candidate approach to seek to identify binding partners for Atf5 in the olfactory epithelium.

RNA-seq from sorted developmental populations of the MOE show dynamic expression of a number of genes within the Cebp family (**Figure 10a**), the most highly expressed of which is Cebpγ. Cebpγ has been demonstrated to heterodimerize with Atf4 and Cebpγ proteins to regulate genes involved in oxidative stress[104] and cellular senescence[105]. Additionally, Cebpγ has been shown to regulate key liver enzymes in coordination with Atf5[106], and is highly co-expressed together with ATF5 in neurons of the vomeronasal organ[107]. We see similar high expression of Cebpγ in the MOE (**Figure 10a,b**), suggesting a potentially cooperative role with Atf5.

To address the importance of Cebpγ in the olfactory system, we analyzed the MOE of mice in which Cebpγ has been genetically ablated. By immunofluorescence staining for the mature marker Adcy3, we see a severe reduction in the number of mature neurons in the tissue, similar to Atf5 KO **(Figure 10c, 5b**). RNA-seq from this tissue shows a drastic reduction in the expression of key developmental marks, suggesting a loss of cellularity that is established by the iOSN stage of development (**Figure 11d,e**). OR transcription is also extremely reduced, with 700 OR genes

significantly downregulated (**Figure 10f,g**). Thus, analysis of the expression of developmental markers and OR genes suggest Cebpγ KO phenocopies the Atf5 KO.

To assess whether Cebpγ is a cofactor for Atf5, and whether this may explain the similar phenotypes observed, we performed ChIp-seq for Cebpγ in whole MOE. We find that Cebpγ binds ~5 fold more sites in the genome as compared to Atf5, which includes a superset of our Atf5 binding sites in MOE (**Figure 11a,c**). While the most significant motif identified from all Cebpγ peaks shows a palindromic CAAT binding site distinct from the top Atf5 motif, this may reflect the fact that Cebpγ may homodimerize, or heterodimerize with other members of the Cebp family, but is also able to interact with Atf5 at only a fraction of total sites (**Figure 11b, 4b**). Indeed, a large portion of Atf5 dependent genes are also Cebpγ dependent (**Figure 11h**), indicating that Cebpγ may heterodimerize with Atf5 to direct proper targeting to these sites.

To address the potential for cooperative binding between Cebpγ and Atf5 proteins, we performed reciprocal ChIp-seq experiments for Cebpγ and Atf5 in both the Cebpγ KO and Atf5 KO mutants. We find that in the absence of Atf5, Cebpγ can still be detected in Atf5 peaks. In contrast, in Cebpγ KO MOE, we lose ChIp signal using either Atf5 or Cebpγ antibodies, indicating that Atf5 binding to its cognate sites requires Cebpγ (**Figure 11i**). This observation provides evidence that Cebpγ recruits Atf5 or stabilizes Atf5 protein at its natural binding sites, and that Cebpγ alone cannot transcriptionally activate Atf5 dependent genes. Importantly, the loss of Atf5 binding in Cebpγ KO mutant is likely not due to loss of expression of Atf5, as Atf5 can still be detected by immunofluorescence (**Figure 11e**).

The demonstrated non-symmetric dependence of Atf5 protein on Cebpγ to target Atf5-specific binding sites may represent a key to the regulatory logic that allows Atf5 target genes to

be transcriptionally activated only in olfactory sensory neurons. Atf5 binding may be constrained by the presence of requisite binding partners, that allows Atf5 targets to be turned on only in the cellular context in which is important to turn on OSN specific genes. At the same time, that Atf4 in the Atf5 Swap mutant cannot replace the function of Atf5 makes sense: inappropriate activation of Atf5 targets by the paralogous stress response transcription factor, Atf4, would prevent Atf5 target genes from aberrantly turning on in cases where the cell experiences an inappropriate source of cellular stress.

In order to explore the sufficiency of Atf5 and other cofactors to bind Atf5 dependent genes, we sought to generate a cell culture system in which both Atf5 and Cebpγ translation can be induced. Histidinol (HisOH) treatment of mouse embryonic fibroblasts (MEFs) has been shown to lead to increased Atf4 and Cebpγ expression[104]. Histidinol is a precursor in histidine biosynthesis and acts as an inhibitor of protein synthesis. As such, it acts as a potent activator of the stress response through phosphorylation of eiF2a.

ChIp-seq from HisOH treated MEFs demonstrated increased binding of the transcription factors Atf4, Atf5 and Cebpγ(**Figure 12a**). In contrast to the MOE in which we detect ~600 Atf5 binding sites, in HisOH treated MEFs, we find more than an order of magnitude increase in the number of ChIp-seq peaks, despite using comparable amount of chromatin as input. This may reflect the fact that Atf5 translation is developmentally restricted in the MOE, while Atf5 is translated synchronously in our cell culture system. GO analysis for Atf4 an Atf5 bound genes consequentially reveal similar GO biological processes (**Figure 12b**). These genes are significantly involved in the regulation of apoptotic signaling pathways, a consequence of prolonged cellular stress. Interestingly, these GO terms do not include those revealed by Atf5

target genes obtained from ChIp-seq performed in the MOE, indicating that Atf5 targets are cell type specific.

The requirement for Cebpγ to recruit or stabilize Atf5 to its targets in the MOE may also be cell-type specific. To ask whether this same dependence operates in our heterologous system, we generated isogenic MEFs from Cebpγ WT and KO embryos. Cebpγ KO MEFs have been previously shown to demonstrate poor proliferative capacity and increased senescence due to a sensitivity to oxidative stress. ChIp-seq for Atf4, Atf5 and Cebpγ was performed on chromatin prepared from both HisOH treated WT and Cebpγ KO MEFs. Both Atf5 and Cebpγ show significant decrease of ChIp-seq signal at Cebpγ bound sites (**Figure 12c**), suggesting that Atf5 may be dependent on Cebpγ to be stably localized to DNA even in MEFs. In contrast to the reduced Atf5 ChIp-seq signal in Cebpγ KO MEFs, Atf4 binding is not significantly reduced. This suggests that, unlike Atf5, Atf4 is able to homo- or heterodimerize with other transcription factors to localize to these sites.

Comparing the Atf5 peaks obtained from the MOE and our cell culture system allows us to ask whether Atf5 binding sites are cell type specific. We find that, although the peak set obtained from HisOH treated MEFs is more numerous, only a fraction of Atf5 peaks are shared between the two. About half of Atf5 peaks obtained from the MOE is shared in MEFs (314), while we observe 315 peaks unique to the MOE and 8,145 peaks unique to MEFs (**Figure 13 a,b**). These MOE unique peak sets may be associated with genes that play critical and OSN specific functions. To look at properties of these binding sites that may direct Atf5 to OSN specific genes, we did a motif analysis, and found that the top motif was strikingly similar between MOE unique peaks and MEF unique peaks (**Figure 13 c,d**). Next, we explored the idea that Atf5 coordinates binding with other MOE specific cofactors. Motif analysis of secondary motifs (i.e. motifs excluding the top

hit), identified binding sites for distinct sets of transcription factors between the two systems. Interestingly the top secondary motifs identified from the MOE unique peak set reveals an enrichment for binding sites associated with Ebf and Lhx2, transcription factors with known critical roles in the olfactory system (**Figure 13e**).[72,76]. In addition to enriching for Ebf and Lhx2 binding sites, we also find that Atf5 peaks identified in the MOE is also bound by these transcription factors the MOE, but that Ebf and Lhx2 does not bind MEF-identified Atf5 peaks in the MOE (**Figure 13f**).

Thus, Atf5 cell-type specific binding may be mediated, at least in part, by the cohort of cofactors present. Ebf and Lhx2, as well as Cebpγ, may collectively direct Atf5 to OSN-specific genes that are critical for proper neuronal function (**Figure 13h**). Additionally, we find that Ebf and Lhx2 are stably bound to these sites even in the absence of Atf5 (**Figure 13g**), similar to the relationship between Cebpγ and Atf5. This collection of cofactors, then, is likely present on Atf5 sites before the initiation of UPR. At the onset of Atf5 translation, Atf5 binding sites would already be decorated by the requisite trans-factors that direct stable association of Atf5 to OSN-specific targets sites, ensuring specificity of Atf5 binding.

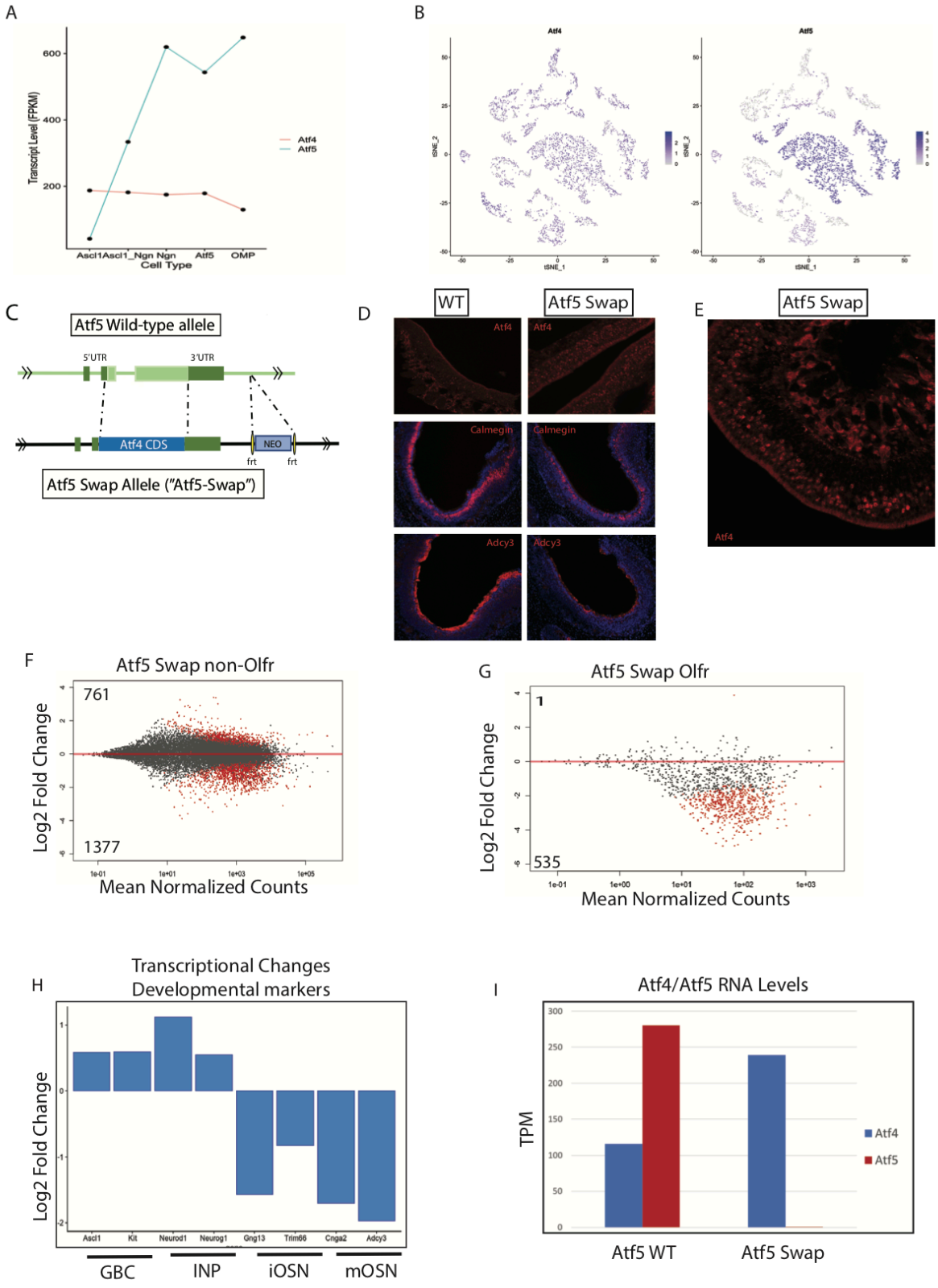

Figure 8. Atf5 Swap phenocopies Atf5 KO

Figure 8. Atf5 Swap mouse phenocopies Atf5 KO in terms of developmental arrest and loss of OR expression

(A) Absolute transcript levels of Atf5 (red) and Atf4 (blue) in different developmental stages of neuronal development; cell types were sorted and RNA-seq libraries were prepared from each population in duplicate (see Figure 1g).

(B) Single cell RNA-seq data from WT whole MOE showing log transformed counts from normalized data.

(C) Atf5 Swap Allele, which replaces the Atf5 coding sequence with Atf4.

(D) Immunofluorescence of Atf4 and a marker of mature neurons, Adcy3 and Calmegin, in Atf5 Swap MOE and control.

(E) Atf4 protein in the Atf5 Swap show an unusual expression pattern which persists into the apical layers of the MOE.

(F) RNA-seq from Atf5 Swap compared to WT control showing differential expression of all non-OR genes. Genes that are significantly differentially expressed are shown in red (FDR < 0.025).

(G) RNA-seq of all OR genes in Atf5 Swap MOE

(H) Log2 fold change in expression for a number of developmental markers that define neuronal lineages.

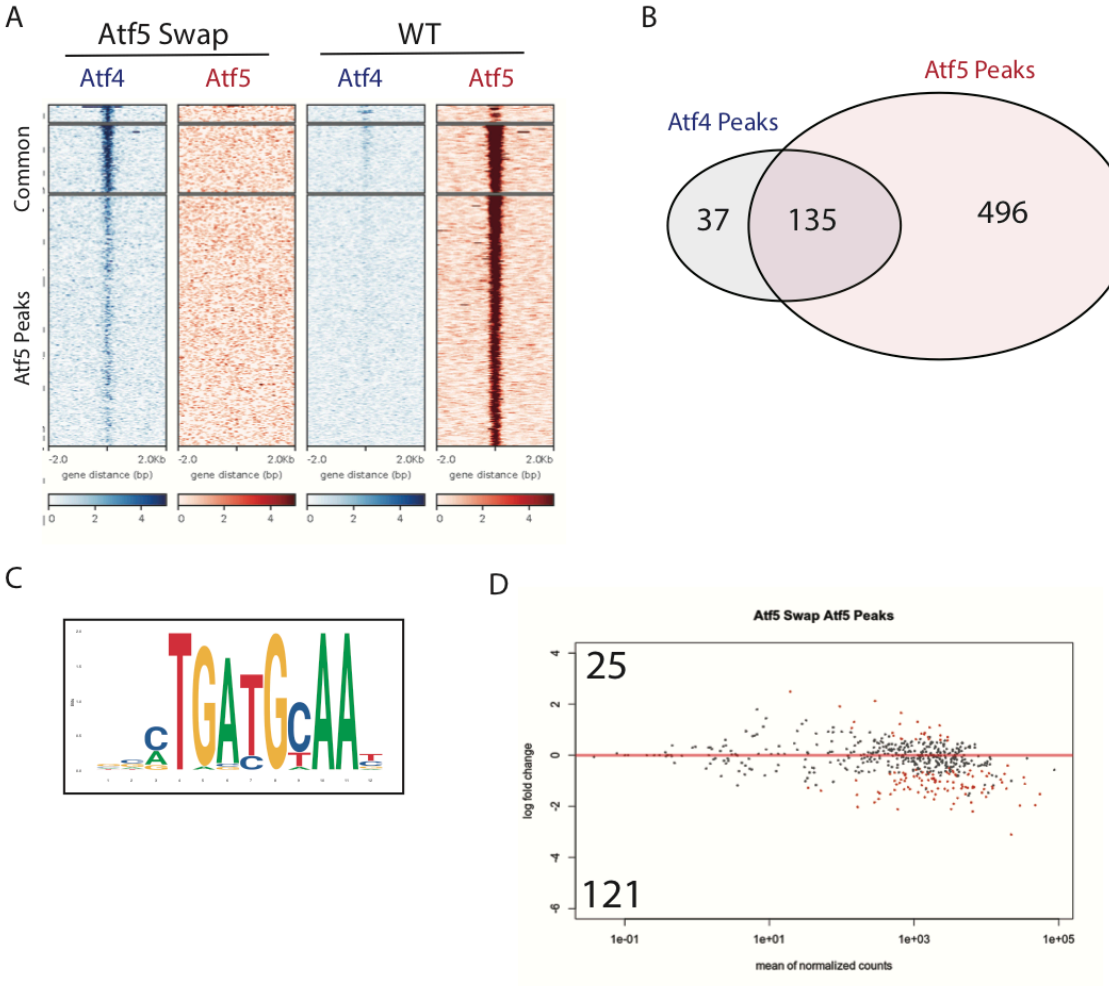

Figure 9. Atf4 ChIp-seq in Atf5 Swap MOE

Figure 9. Atf4 ChIp-seq in Atf5 Swap MOE

(A) Atf4 and Atf5 ChIp-seq signal from Atf5 Swap or WT MOE. The genomic regions are parsed into peaks that are uniquely identified in Atf4 ChIp-seq from the Atf5 Swap mouse (top, 37 loci), are common binding sites for Atf4 in the Atf5 Swap as well as Atf5 in WT MOE (middle, 135 loci), or are unique Atf5 binding sites in WT MOE (bottom, 496 genes).

(B) The overlap of loci that are bound by Atf4 in Atf5 Swap MOE, or Atf5 in WT MOE. Peaks are called using HOMER, with FDR < 0.001.

(C) Top motif obtained by all Atf4 peaks identified in Atf5 Swap (172 sites total).

(D) Differential expression of Atf5 peak genes from RNA-seq performed in Atf5 Swap MOE.

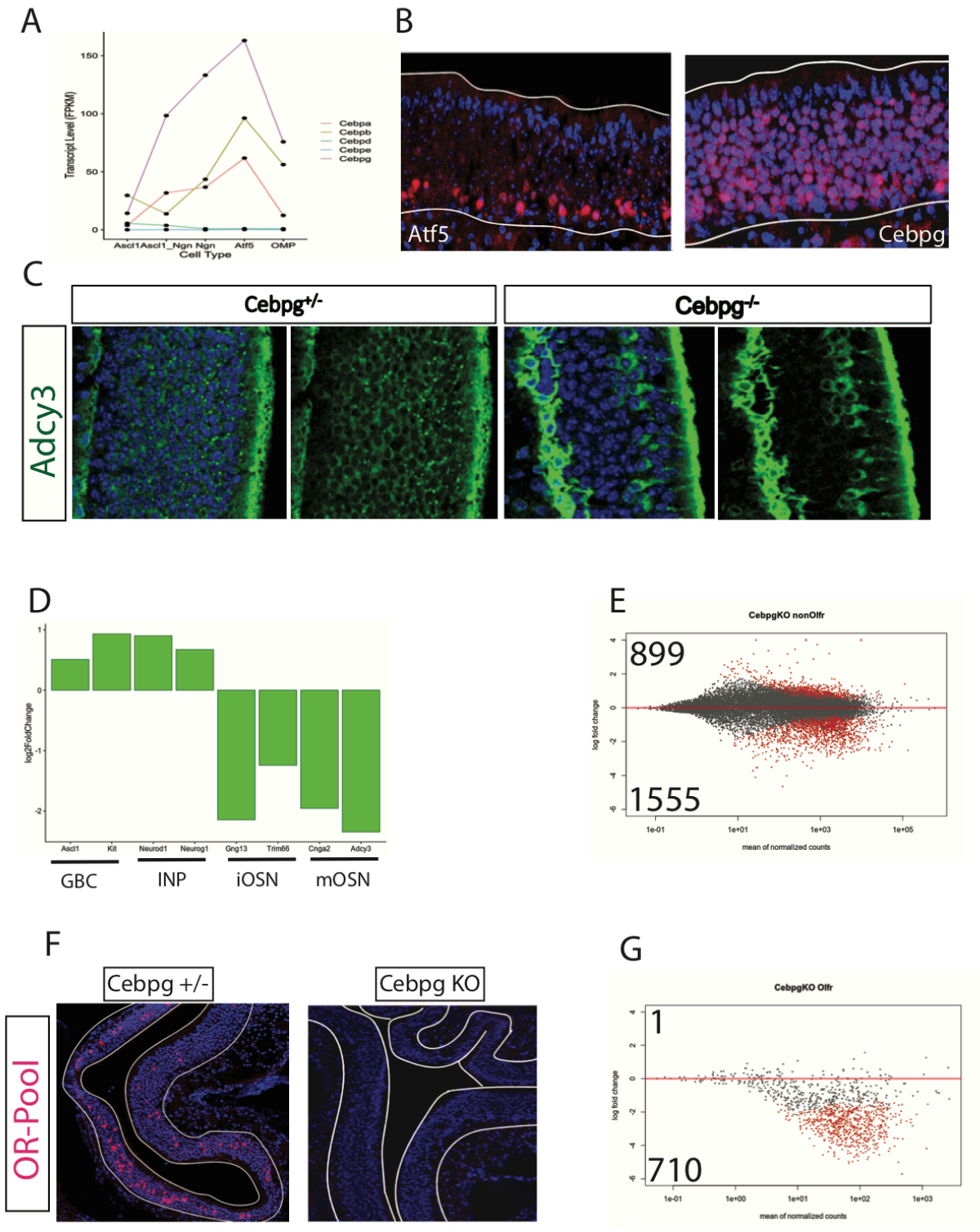

Figure 10. Cebpγ KO phenocopies Atf5 KO

Figure 10. Cebpγ KO Phenocopies Atf5 KO

(A) Expression levels of various Cebp family members at different developmental stages of the MOE, from RNA-seq experiments performed on sorted populations.

(B) While Atf5 protein is localized to the more basal regions of the epithelium Cebpγ is detected throughout the tissue.

(C) Staining for the mature OSN marker Adcy3 shows a drastic reduction in the number of immunopositive cells in the Cebpγ KO mutant**.**

(D) Log2 fold change in transcript levels for a handful of developmental markers between Cebpγ KO and control MOE.

(E) MA plot showing changes in expression of all Non-OR genes (significant genes, in red, have FDR < 0.025)

(F) MA plot showing changes in expression for all OR genes

(G) IF for a pool of antibodies directed against OR proteins

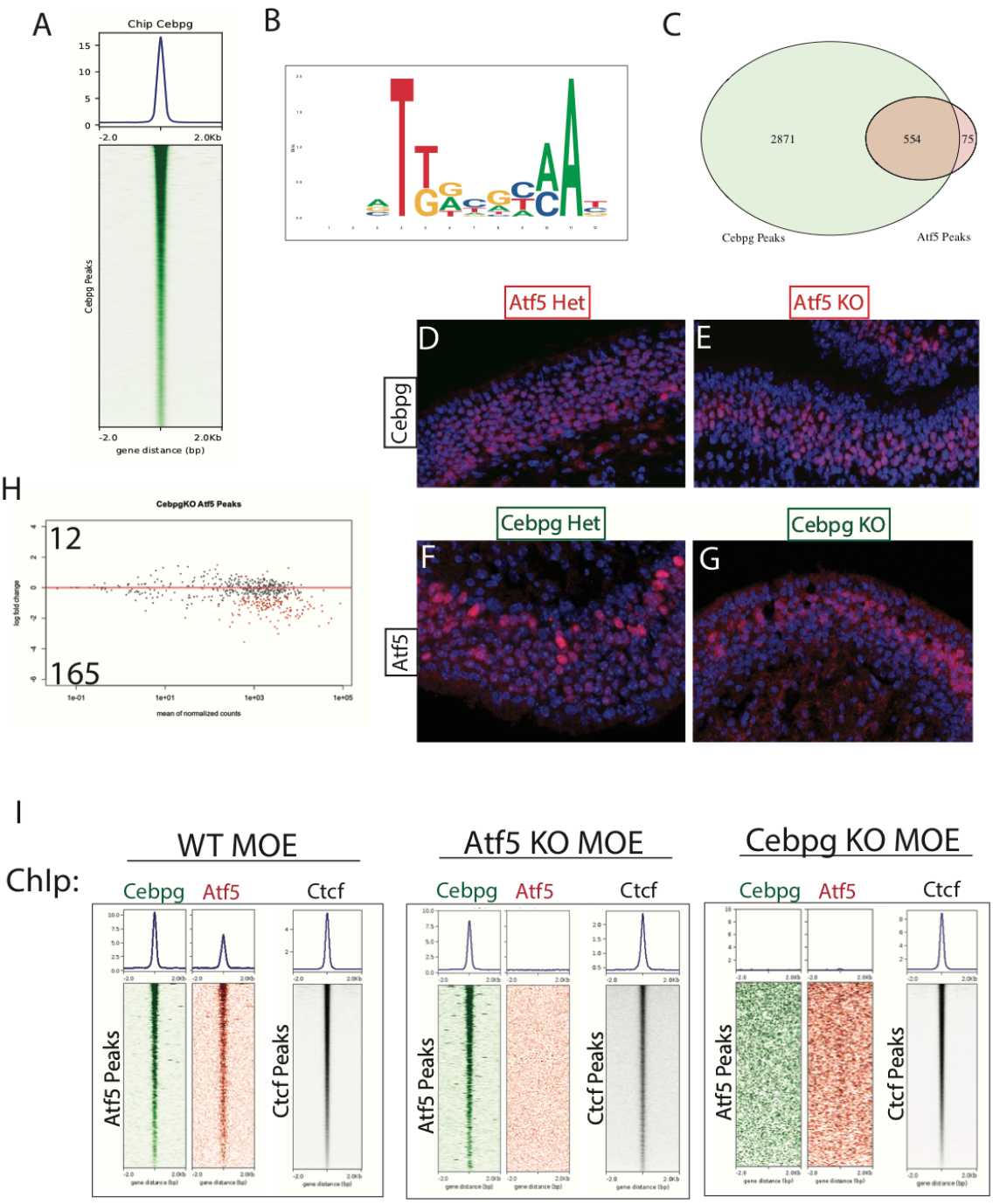

Figure 11. Atf5 depends on Cebpγ to bind DNA, but not for expression

Figure 11. **Atf5 depends on Cebpγ to bind DNA, but not for expression**

(A) Meta plot summarizing the signal from ChIp-seq experiment using antibody against Cebpγ from whole MOE. Peak regions are those identified by HOMER (FDR < 0.001)

(B) Top motif logo obtained from Cebpγ peak set

(C) Venn diagram showing the overlap of peaks identified from Cebpγ ChIp or Atf5 ChIp experiments**.**

(D-G) IF of the MOE of control (D,F) or Mutant (E,G) mice bearing the indicated mutation. Staining for either Cebpγ (D,E) or Atf5 (F,G)

(I) Reciprocal ChIp-seq experiments from control, Atf5 KO MOE or Cebpγ KO MOE using antibodies against Cebpγ or Atf5. Metaplots in green and red show ChIp signal at Atf5 consensus peak sites. As a control, Ctcf ChIp-seq experiments were performed in parallel using the same chromatin prepared from the appropriate genotype, visualizing the Ctcf signal on known Ctcf binding sites.

A

ChIp-seq Peaks

	Atf4	Atf5	Cebpg
DMSO-Treated MEFs	54	47	4126
HisOH-Treated MEFs	7585	8459	7328

B

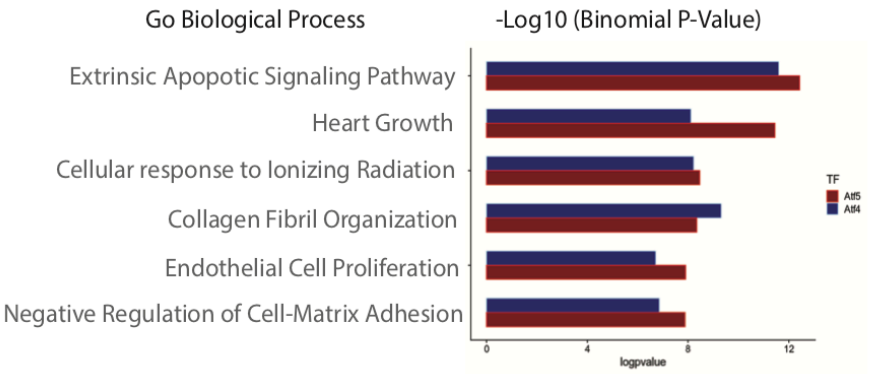

C

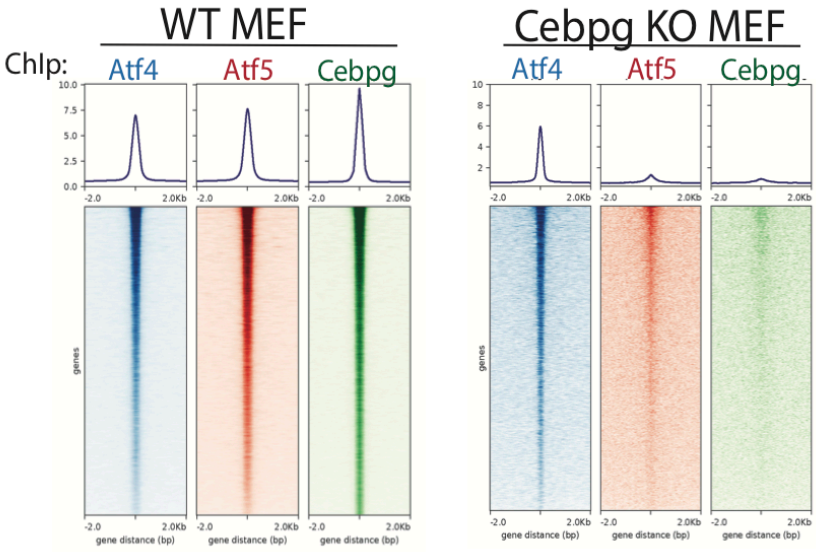

Figure 12. Atf4 and Atf5 ChIp-seq from HisOH treated MEFs

Figure 12. Atf4 and Atf5 ChIp-seq from HisOH treated MEFs

(A) HisOH treated MEFs induce binding of the transcription factors Atf4 and Atf5

(B) GO analysis of binding sites for Atf4 and Atf5 in HisOH treated MEFs

(C) Chip for Atf4, Atf5 and Cebpγ in WT and Cebpγ KO MEFS

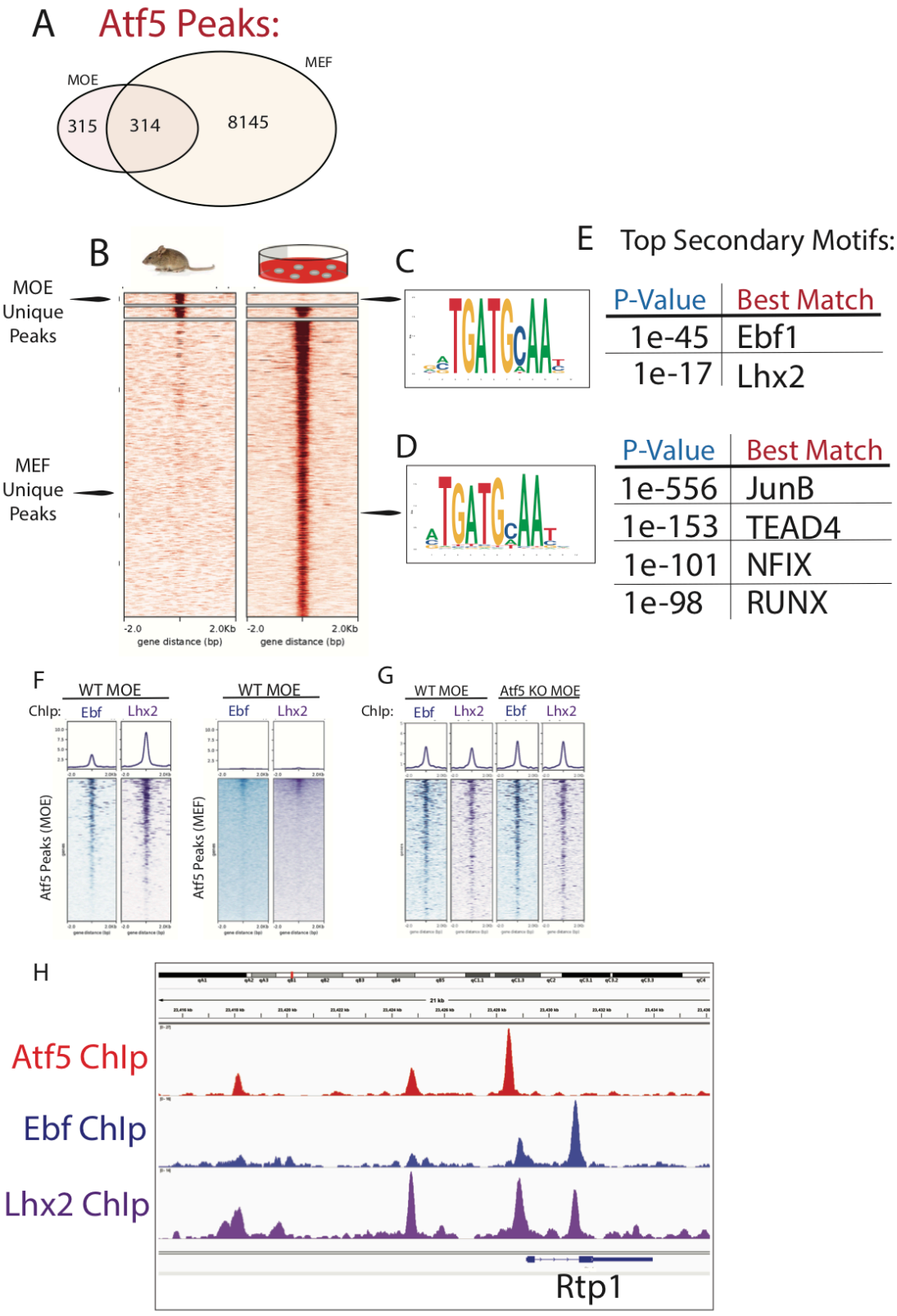

Figure 13. Atf5 binding sites are co-bound with Ebf and Lhx2 specifically in the MOE

Figure 13. Atf5 binding sites are Co-bound with Ebf and Lhx2 specifically in the MOE

(A) Venn Diagram showing the overlap of Atf5 peaks identified from MOE or HisOH treated MEFs

(B) Metaplot showing the ChIp-seq signal from MOE (left) or MEFs (right), parsing the genomic regions into either MOE-unique (top), common peaks (middle), or MEF-unique (bottom).

(C) Motif Logos for top identified motifs from either the MOE unique or

(D) MEF unique peak sets.

(E) Motif analysis from MOE Unique peaks, showing the second and third top matches (top) or Motif analysis from MEF unique peaks, showing the 2-5 top matches

(F) Ebf and Lhx2 ChIp-seq from MOE, looking at signal from all Atf5 peaks identified in the MOE (left), or Atf5 peaks identified in MEFs (right)

(G) Ebf and Lhx2 ChIp-seq from WT (left) or Atf5 KO MOE (right), displaying Atf5 consensus peak set obtained from MOE

(H) Gene track showing Atf5, Ebf, and Lhx2 ChIp-seq signal from MOE at the Rtp1 locus

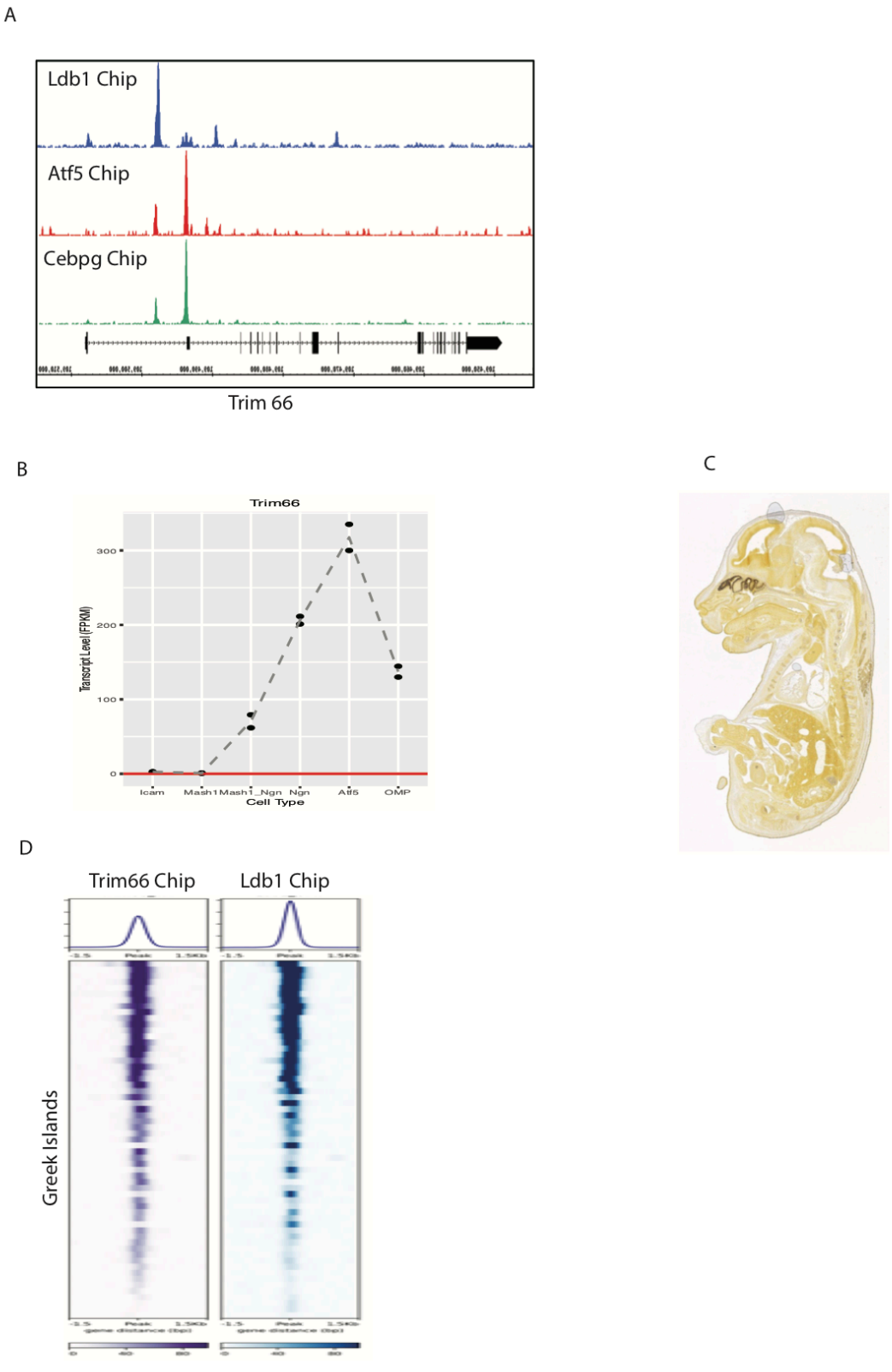

Figure 14. Trim66 as a candidate Atf5 dependent gene involved in Greek Island Regulation

Figure 14. Trim66 as a candidate Atf5 dependent gene involved in Greek Island Regulation

(A) Trim66 is bound by Atf5, Cebpγ and Ldb1. Gene tracks showing ChIp-seq signal at Trim66 gene for Atf5, Cebpγ and Ldb1. Atf5 and Cebpγ ChIp-seq experiments were performed on chromatin prepared from whole MOE, while Ldb1 ChIp-seq was performed on Omp-GFP^{+} sorted mOSNs[76].

(B) Transcript levels for Trim66 in sorted populations of the MOE. Trim66 is highly expressed in Atf5^{+} cells.

(C) RNA-is for Trim66 show specific expression in embryonic MOE (Allen Developing Mouse Brain Atlas)

(D) ChIp-seq signals for Trim66 and Ldb1. Genomic regions are the Greek Islands. Trim66 ChIp was performed on whole MOE, Ldb1 ChIp was performed on Omp-GFP^{+} sorted cells (mOSNs).

Discussion / Future Directions

Atf5 Translation is induced by singular rather than polygenic OR transcription

Given the evidence that OR expression is necessary and sufficient for Atf5 translation[84], we sought to gain insight into when UPR is engaged in OSNs, and to answer whether early polygenic OR expression, or later singular OR acts as the signal that triggers it. Using a novel Atf5 reporter that is only translated as cells are engaged in UPR, we first addressed the question when Atf5 protein is expressed developmentally, and found that these cells represent the iOSN stage of development.

By performing single cell RNA-seq on whole MOE, as well as bulk RNA-seq on sorted INP and iOSN populations, we provide evidence that high level monogenic OR transcription can be detected before the induction of UPR, supporting the model that singular OR choice precedes and provides the signal that engages UPR. Consistent with other reports[56,57,89], we also observe a drastic increase in total OR transcription between cells that display early polygenic OR transcription compared to later stages of development. These results suggest that the high transcriptional output of the dominant, "chosen" OR allele may serve as the signal that activates the UPR by overwhelming protein processing capacity in neuronal progenitor cells. Additionally, as part of its non-canonical role in the MOE, we find that Atf5 binds to and upregulates the expression of olfactory specific chaperone proteins and OR coreceptors, including RTP1 and RTP2, consistent with a model in which early polygenic OR transcripts cannot be successfully translated and processed until Atf5 targets are expressed. This also provides an explanation for how UPR is ultimately resolved in mature OSNs.

Given that UPR is deployed only after dominant OR expression is achieved, the rules that govern the permissiveness of early polygenic OR expression, and the mechanisms that restrict the

OR repertoire expressed during development, must be Atf5 independent. What could explain promiscuous transcriptional activation of multiple OR alleles? As ORs bear post-translational modifications indicative of silenced genes (H3K9me3 and H4K20me3), and downregulate LBR before the INP stage of development[66,67], polygenic OR expression cannot be explained by the absence of heterochromatinization or compaction of OR genes globally. Additionally, ORs that are co-expressed during this early stage come from multiple chromosomes, indicating that it is not the result of the targeted accessibility of a specific locus that permits polygenic OR expression[57]. Instead, polygenic OR expression may be afforded by the continued availability of Lsd1, which remains highly expressed in neuronal progenitor cells[81]. As a de-repressor of OR genes, and a potential target of OR-induced feedback, Lsd1 plays an integral role in OR activation. In agreement with experimental results, singular OR expression can be modeled by a slow process of H3K9 demethylation by Lsd1, followed by its swift downregulation[83]. Indeed, lineage tracing has shown that neuronal progenitors take ~5 days to transition to the iOSN stage, Lsd1 mediated de-repression of multiple ORs may be taking place. Interestingly, Lsd1 remains highly transcribed in iOSNs (data not shown), consistent with an additional role in $Atf5^{+}$ cells after dominant OR expression is observed. This may be required to facilitate the serial OR vetting process, which results in an increase in OR gene-switching in the absence of Atf5.

In the absence of feedback mechanisms, how does incipient polygenic OR expression transition to dominant OR expression in INP cells? DNA/RNA FISH experiments, as well as proximity ligation assays have shown that Greek islands form an interchromosomal hub in a developmentally regulated way, and that in mature OSNs, Greek islands converge and cover the actively transcribed OR allele, facilitating singular robust expression[67,73,73]. Importantly, these interactions are highly reduced in INP cells, thus, promiscuous Greek island-OR contacts in

neuronal precursor populations may allow polygenic OR expression, and as the Greek island hub forms, expression of a dominant OR prevails. Here, we provide evidence that singular OR expression signals for Atf5 translation by characterizing the nuclear architecture of cells before, during and after this transition. By Hi-C, we find OR compartments and the Greek island hub appear fully formed by the iOSN stage, and that this does not require Atf5 to do so, consistent with the model that UPR is initiated after singular OR selection is realized.

It appears, then, that Atf5 participates in stabilizing OR expression during the serial vetting process which occurs during the iOSN stage; when Atf5 is absent, an increase in OR "gene-switching" is observed[79,84]. How does Atf5 accomplish this? One possibility is that although Atf5 is not required for the formation of OR gene compartments and Greek island hubs, it may play a role in the maintenance of these structures. Although the number of mature OSNs in the Atf5 KO is drastically reduced, it may be possible to address this by Hi-C in this sparse population.

As Atf5 protein is absent in OR clusters by ChIp-seq, and is not significantly enriched on Greek islands, it is likely that stable OR expression is enforced by one or more downstream targets of Atf5. Using single cell RNA-seq we were able to identify the temporal regulation of gene expression changes among Atf5 target genes, and we find that some of the 'first responders' include chromatin modifying enzymes associated with repression, such as Cbx4 and Trim66 (**Figure 7**). Cbx4 is a component of the polycomb repressive complex (PRC1), as well as a SUMO E3 ligase. Cbx4 has been shown to play diverse roles in gene expression by epigenetic gene silencing via recruitment of the PRC1 complex to specific loci, or by modulating the activity of other transcription factors by post-translational modifications. These roles have been shown to be critical for the establishment and maintenance of cell identity in a number of different systems. For example, Cbx4 has been demonstrated to maintain proper epithelial transcriptional program

by repressing non-epithelial genes[108]. In hematopoietic stem cells, Cbx4 has been implicated in promoting a pro-differentiation phenotype[109]. We find that in the olfactory epithelium, Cbx4 binds directly to the neuronal progenitor gene, Ngn1, by ChIp-qPCR (Data not shown). This observation may indicate that, in addition to a role in promoting maturation, Atf5 may also downregulate genes associated with the neuronal progenitor state. In support of this hypothesis, we find that transcription of genes associated with the GBC/INP stages of development appear upregulated in the various mutants we describe in this paper. This may be a critical determinant in regulating developmental changes in OSNs that prevent co-expression or increased gene-switching of ORs in mature OSNs.

Another compelling model for the stabilization of OR expression involves the Atf5 target gene, Trim66, which is specifically expressed in olfactory tissue, and is highly upregulated coincident with Atf5 translation (**Figure 14**). Trim66 is a member of the TIF1 family of cofactors which contains an N-terminal RBCC domain, a C-terminal PHD finger/bromodomain, and has been shown to bind to HP1 proteins[96]. We find by ChIp-seq that Trim66 binds ~2000 genomic regions, 10% of which are distributed across OR clusters and Greek islands. This lends itself to the exciting hypothesis that Trim66 may be involved in regulating the interaction frequencies between OR enhancers and OR genes, leading to the stabilization of the chosen OR. This may be accomplished by "locking in" the Greek island hub and the expressed OR allele physically for the life of the neuron. Alternatively, Trim66 may be exerting a repressive function on the Greek islands that are not engaged with the chosen OR, preventing spurious transcriptional activation of all other OR genes. Greek islands are bound by Lhx2 and EBF proteins[72], which synergistically recruit the Lim domain binding protein, LDB1. LDB1 is involved in long range DNA interactions, and by ChIp-seq, is strongly enriched on Greek islands[76]. Moreover, genetic ablation of LDB1 in mature

OSNs demonstrates that the stable expression and continued interaction frequency of the chosen OR with the Greek island hub requires LDB1. Interestingly, the expression of LDB1 is modulated by ubiquitination[110], and one Trim66 related protein, Trim33, had been shown to decrease the expression of LDB1 in a manner that requires its N-terminal Ring domain[111]. Collectively, these observations offer a model in which Trim66 may modulate the stability of LDB1 proteins that are not engaged with the actively transcribed OR allele. Considering that that chosen OR physically interacts with a Greek island hub within the euchromatic territory of the nucleus[67,73,76], yet Trim66 can interact with heterochromatic proteins, Trim66 may preferentially prohibit the activity of Greek islands that are not engaged with the active OR allele, either through the destabilization of LDB1 protein, or through its deacetylase activity on chromatin.

Atf5 as an organizer of OR trafficking, OSN differentiation, and axon growth

By taking advantage of a translational control mechanism that is more widely reserved for the cellular stress response, Atf5 is well-equipped to handle swift transcriptional changes in response to the critical moment of singular OR transcription. One of the most highly transcribed genes in olfactory neurons, Atf5 can ably detect OR protein through the UPR, and enforce a developmental regime change that not only locks in the chosen OR, but also allows proper neuronal maturation and function. By ChIp-seq and RNA-seq in Atf5 mutant mice, we were able to find 200 Atf5 dependent genes involved in a number of critical processes including OR protein processing, axonogenesis and ER homeostasis. In addition to its direct targets, Atf5 likely has many indirect downstream effects through the activation of various identified transcription factors and chromatin modifying enzymes.

What is noticeably missing as a target of Atf5 is Adcy3, the presumed sensor of OSN maturation that has been shown to downregulate Lsd1, which would substantiate the "feedback" signal that leads to the stable expression of the chosen OR. Instead, Adcy3 may be an indirect target of Atf5.

An emerging but unanswered question from these studies is the observation that Atf5 dependent genes remain highly transcribed in mature neurons (**Figure** 5g). In these cells, we notice a drastic decrease in Atf5 immunoreactivity, despite the fact that Atf5 transcription remain high as well (**Figure 1c, 8a**). One possible explanation for this is Atf5 has the ability to alter the epigenetic landscape of its target genes, in a way that persists once UPR has been resolved, and that allows transcriptional activation of its targets in its absence. Contrary to this hypothesis, we have observed no differences in a number of chromatin marks assayed at these sites between WT and Atf5 KO MOE (**Data not shown)**. Alternatively, Atf5 may lead to the transcriptional activation of another bZIP transcription factor that can replace the function of Atf5, but that is not itself under the same translational control restrictions as Atf5. One possibility is Creb3l1, a cAMP response element binding protein that has been shown to be activated by ER stress[112,113]. Finally, it is possible that Atf5 is translated, though at undetectable levels, in mature OSNs, and remain stably bound to the ~600 target sites in the genome. One way to address this possibility is to ablate the UPR sensing machinery specifically in mature OSNs. We are currently crossing a conditional Perk flox/flox allele with a mature OSN-specific recombinase, Omp-CRE. This would allow us to identify any potential role that low level Atf5 translation may have in mature neurons.

Atf5 is recruited by Cebpγ to Lhx2 and Ebf bound sites

We identify ~600 Atf5 bound sites in OSNs, which are co-occupied by the transcription factors Cebpγ**,** Lhx2 and Ebf. Further, Cebpγ is required for the recruitment of Atf5 to DNA, likely through heterodimerization, and this property is shared in a heterologous cell system. The specificity of this interaction is highlighted by the fact that Atf5 does not appear co-bind with other members of the Cebp family in either MOE or MEFs, as evidenced by its inability to be recruited to its genomic targets when Cebpγ is genetically ablated. In contrast, Atf4 binding persists in Cebpγ KO MEFS. Cebpγ/Atf5 may also play an important role in the vomeronasal organ, an olfactory subsystem[107,114].

Lhx2 and Ebf family proteins play critical roles in specifying OSN identity and OR expression. Lhx2 and Ebf co-bind with stereotypical spacing at Greek islands, and Lhx2 is required for the formation of OR cluster interactions in INP cells. Ldb1, an interaction partner of Lhx2, affords long range DNA interactions and is required for the formation of Greek islands[76]. Thus, the Lhx2, Ebf, Ldb1 complex plays important roles in the formation of OSN specific nuclear compartments.

Atf5 binding sites are also enriched for Ldb1, and from our Hi-C analysis we find that these regions exhibit significant frequency of interaction that is developmentally regulated and Ldb1 dependent (data not shown). Interestingly, we find that these long-range interactions are not Atf5 dependent. This provides a model in which Cebpγ, Lhx2, Ebf and Ldb1 are already poised at Atf5 target sites *before* the onset of Atf5 translation; once OR-induced Atf5 translation commences, the transcription factor can be swiftly directed to its target sites, which are already concentrated within the nucleus.

In addition to known chaperones (Rtp1, Rtp2, Ric8b, Gnal), Atf5 targets likely include other genes that can facilitate OR surface expression and function in heterologous systems. Reconstituting Atf5 activation of OSN specific targets in cell culture would provide an excellent way to express ORs for studies that could reveal OR-ligand specificities, or produce OR proteins that would afford structural analysis. Atf5 and Cebpγ, though, are not sufficient to activate these targets in other cell types (MEFs); but through the coordinated actions of Lhx2 and Ebf together, we may be able to accomplish this. Accordingly, we are working to produce a stable cell line that could inducibly express these critical OSN transcription factors.

Non-redundant functions between Atf5 and Atf4

The retooling of a stress-response transcription factor for olfactory system development offers interesting insight into the special nature of the system. The atypical translational regulation of Atf5 links its role as a sensor of high level OR expression to the quick transcriptional changes that accompany OSN development. This property of a stress response transcription factor may be employed in other cell types as well in controlling development and differentiation in other tissues. The liver, for example, expresses Atf5 at high levels[115], and ectopic delivery of Atf5 leads to an increase in hepatic genes that is enhanced by interaction with constitutive androstane receptor. In conjunction with other transcription factors, ectopic Atf5 expression promotes the transdifferentiation of human stem cells to exhibit a hepatic-like phenotype[116,117]. In pancreatic β-cells, Atf5 has been shown to provide a pro-survival function under stressed conditions. Considering that both of these cell types endure high levels of protein output it is possible that the use of Atf5 as a developmental regulator in such cases is tied to the requisite burden of protein production.

In the brain, Atf5 has been shown to be important for the proper development and differentiation of a number of cell types as well. Atf5 is highly expressed in neural precursor cells of the ventricular zone (VZ) as well as the subcentricular zone (SVZ), and as is the case in the MOE, its expression becomes restricted in mature, postmitotic neurons and astrocytes[118–121]. Overexpression Atf5 or delivery of a dominant-negative form of Atf5 confirms that the suppression of Atf5 is important to exit the proliferative state, and to terminally differentiate into neurons, as well as oligodendrocytes and astrocytes.

The Atf5 paralogue, Atf4, is more ubiquitously expressed, and has been widely studied for its cytoprotective functions. Yet, Atf4 has also been implicated in having a role in the proper development of a number of tissues as well. Atf4 knock out mouse models demonstrate a defect in the production of anterior lens epithelial cells during embryonic development due to p53 dependent apoptosis[122,123]. Genetic ablation of Atf4 also leads to severe anemia due to a reduction in the self-renewal and proliferation of hematopoietic stem cells (HCSs) in the fetal liver[124,125]. This phenotype appears to be due to increased apoptosis and decreased expression of key genes that support HSCs by surrounding niche cells.

Despite similar translational control mechanisms via cryptic upstream open reading frames, as well as nearly identical DNA binding motifs, Atf4 and Atf5 seem to play roles in the proper development of diverse and non-overlapping cell types. What may account for the non-redundant functions of these stress response transcription factors. First, it may be the case that the expression of these genes may be distributed in a nonequivalent fashion. Alternatively, their expression levels may be disparate within the same tissue. Indeed, this is the case in the MOE, wherein higher Atf5 expression is more dynamically regulated, and restricted to a particular set of cell types in comparison to Atf4. We find, though, that replacing the endogenous Atf5 gene with

Atf4 does not rescue the developmental phenotype we observe in the Atf5 knock out. This is despite the fact that this genetic manipulation increases Atf4 transcript levels to that of wild type Atf5 levels. An alternative explanation for non-redundant functions of these genes is that they engage in unique homo- or heterotypic interactions. Atf4 and Atf5 share 55% identity within their leucine zipper domains, and Atf5 has a proline-rich region, which is hypothesized to influence the transactivation properties of this protein[126]. Although Atf4 has been shown to heterodimerize with Cebpγ to enact restorative measures in cells challenged with oxidative stress, here, we find that Atf5 has a requisite interaction with Cebpγ that is required for the stable expression of OR genes, and the proper maturation of olfactory neurons, via UPR stress, and this property is not shared with Atf4. Additionally, in a cell culture system in which stress is induced by mimicking amino acid limitation chemically, Atf5 appears to maintain this same requisite dependence on Cebpγ as well. Thus, members of the bZip family of transcription factors form multimeric complexes that are tailored to assist in cell type and stress-signal specific responses; in the MOE, this response leads to stable OR expression and neuronal maturation.

The requirement of Atf5 instead of Atf4 in the olfactory system may have two purposes. First, given that OR genes constitute such a large portion of the genome, the aberrant transcription of them even at low levels in non-olfactory tissue may pose a transcriptional burden that could be problematic to the proper function of the cell. Using a specially dedicated stress-response transcription factor that can uniquely activate a set of OR specific chaperone proteins would prevent the spurious expression of these genes in other tissues. Additionally, the ability of OSNs to distinguish between OR-induced UPR induction, and other cellular stress signals may allow these neurons to distinguish between a developmentally regulated signal, and perhaps a more systemic signal of stress (chemotoxic exposure, for example).

Even when Atf4 is overexpressed, we find it impaired in its binding affinity and specificity to Atf5 specific sites in the MOE. Further, Atf4 binding isn't sufficient for transcriptional activation. A possible explanation for this that we haven't explored is that the two transcription factors provide distinct activities to these binding sites. While both are transcriptional activators, this may be accomplished by distinct mechanisms. We find that an unusual portion of Atf5 binding sites occur in intronic and intergenic regions of the genome, raising the possibility that Atf5 could act in directing alternative splicing/promotor choice, or supporting enhancer-promotor interactions. Additionally, a majority of genes bound by Atf5 are not affected in Atf5 KO MOE, indicating that Atf5 binding alone is not sufficient for transcriptional activation. Interestingly, this set of binding sites includes nearly half of all tRNA synthetase genes, which are known to be regulated by Atf4 during ER stress, but apparently not by Atf5 during OSN development. The Atf5 binding sites for these genes are characteristically close to their transcriptional start sites, suggesting that Atf5 may have acquired a unique activity distinct from Atf4 during evolution.

The Stress Response and Neural Function

The observation that a highly conserved and widely employed cellular stress response has been co-opted for proper development and gene regulation in the olfactory system prompts the question whether this type of cellular process is utilized in other cell types in the brain. As discussed earlier, Atf5 expression is observed in a number of neural precursor cells, and its timely downregulation accompanies terminal differentiation in these cell types, which includes both glia and neurons. In order to describe the cellular processes and transcriptional changes that accompany development in these cells, and to gain more insight into the role of Atf5 in OSN development, it would be beneficial to isolate and characterize these cells. To this end, we intend to use the novel

Atf5 translational reporter generated for this study to sort Atf5^{+} neurons in mice. Additionally, because the reporter cassette replaces endogenous Atf5, we will be able to glean functional data of the role of Atf5 by using this reagent to isolate cells undergoing cellular stress, but that have both copies of Atf5 removed. This is important because Atf5 has been shown to play roles in proper neural development, as well as in managing the stress response in a way that helps to protect neural cells from a number of disease phenotypes. For example, mouse models for status epilepticus exhibit increased Atf5, which seems to play an anti-apoptotic role[127]. In human brain, a deficiency of soluble ATF5 has been observed in patients with Huntington's disease, accompanied by an accumulation of ATF5 in characteristic polyglutamine nuclear inclusion; overexpression of ATF5 can rescue polyglutamine-induced apoptosis in a cell culture model of Huntington's disease[128]. Recently, continuous activation of the integrated stress response has been observed in models of Down syndrome, leading to a number of disease symptoms that include a deficiency in long term memory and synaptic plasticity.[129] These effects can be attenuated by small molecule inhibitors that prevent the phosphorylation of eif2a, or by enhancing the activity of the eif2 dedicated guanine nucleotide exchange factor, eif2B. Thus, Atf5 has been implicated in proper neuronal development as well as serving a cytoprotective function in a wide array of neural cell types, as well as sensory neurons of the olfactory system. In addition, dysregulation of Atf5 expression and activity has increasingly been shown to be involved in a number of diseases. Accordingly, strategies that can modulate Atf5 function in vivo may have promising clinical uses in understanding and ameliorating a number of human diseases.

Conclusion

Our experiments revealed that Atf5 translation occurs at the onset of singular OR transcription following the formation of a multi-chromosomal enhancer hub, resulting in the direct regulation of ~200 genes with prevailing roles in OR gene trafficking, ER homeostasis, chromatin regulation, and axonogenesis. Interestingly, genetic substitution experiments revealed that Atf4 does not activate most of the Atf5-dependent genes, due to differential specificity for genomic targets. The transcription factor Cebpγ, which is highly expressed in the MOE, directs Atf5 binding towards genomic regions occupied by Lhx2 and Ebf, the master regulators of OSN identity, providing a mechanistic explanation for the selective expression of Atf5 in developing OSNs. Taken together, our experiments provide insight to the relationship between OR gene choice and UPR induction, and reveal how Atf5 translation induces transcriptional changes that facilitate OR trafficking, axon growth, and terminal OSN differentiation.

Bibliography

1. Miller, A. M., Maurer, L. R., Zou, D.-J., Firestein, S. & Greer, C. A. Axon fasciculation in the developing olfactory nerve. *Neural Develop.* **5**, 20 (2010).
2. Cohen, Y., Reuveni, I., Barkai, E. & Maroun, M. Olfactory learning-induced long-lasting enhancement of descending and ascending synaptic transmission to the piriform cortex. *J. Neurosci. Off. J. Soc. Neurosci.* **28**, 6664–6669 (2008).
3. Ferry, B., Ferreira, G., Traissard, N. & Majchrzak, M. Selective involvement of the lateral entorhinal cortex in the control of the olfactory memory trace during conditioned odor aversion in the rat. *Behav. Neurosci.* **120**, 1180–1186 (2006).
4. Kadohisa, M. & Wilson, D. A. Separate encoding of identity and similarity of complex familiar odors in piriform cortex. *Proc. Natl. Acad. Sci. U. S. A.* **103**, 15206–15211 (2006).
5. Belluscio, L., Koentges, G., Axel, R. & Dulac, C. A Map of Pheromone Receptor Activation in the Mammalian Brain. *Cell* **97**, 209–220 (1999).
6. Larriva-Sahd, J. The accessory olfactory bulb in the adult rat: A cytological study of its cell types, neuropil, neuronal modules, and interactions with the main olfactory system. *J. Comp. Neurol.* **510**, 309–350 (2008).
7. Hammen, G. F., Turaga, D., Holy, T. E. & Meeks, J. P. Functional organization of glomerular maps in the mouse accessory olfactory bulb. *Nat. Neurosci.* **17**, 953–961 (2014).
8. Rodriguez, I., Feinstein, P. & Mombaerts, P. Variable Patterns of Axonal Projections of Sensory Neurons in the Mouse Vomeronasal System. *Cell* **97**, 199–208 (1999).
9. Halpern, M. The organization and function of the vomeronasal system. *Annu. Rev. Neurosci.* **10**, 325–362 (1987).
10. Leung, C. T., Coulombe, P. A. & Reed, R. R. Contribution of olfactory neural stem cells to tissue maintenance and regeneration. *Nat. Neurosci.* **10**, 720–726 (2007).
11. Carter, L. A., MacDonald, J. L. & Roskams, A. J. Olfactory Horizontal Basal Cells Demonstrate a Conserved Multipotent Progenitor Phenotype. *J. Neurosci.* **24**, 5670–5683 (2004).
12. Iwai, N., Zhou, Z., Roop, D. R. & Behringer, R. R. Horizontal Basal Cells Are Multipotent Progenitors in Normal and Injured Adult Olfactory Epithelium. *Stem Cells Dayt. Ohio* **26**, 1298–1306 (2008).
13. Cau, E., Gradwohl, G., Fode, C. & Guillemot, F. Mash1 activates a cascade of bHLH regulators in olfactory neuron progenitors. *Dev. Camb. Engl.* **124**, 1611–1621 (1997).
14. Fletcher, R. B. *et al.* Deconstructing Olfactory Stem Cell Trajectories at Single Cell Resolution. *Cell Stem Cell* **20**, 817-830.e8 (2017).
15. Caggiano, M., Kauer, J. S. & Hunter, D. D. Globose basal cells are neuronal progenitors in the olfactory epithelium: a lineage analysis using a replication-incompetent retrovirus. *Neuron* **13**, 339–352 (1994).
16. Huard, J. M., Youngentob, S. L., Goldstein, B. J., Luskin, M. B. & Schwob, J. E. Adult olfactory epithelium contains multipotent progenitors that give rise to neurons and non-neural cells. *J. Comp. Neurol.* **400**, 469–486 (1998).
17. Krolewski, R. C., Packard, A., Jang, W., Wildner, H. & Schwob, J. E. Ascl1 (Mash1) knockout perturbs differentiation of nonneuronal cells in olfactory epithelium. *PloS One* **7**, e51737 (2012).
18. Breipohl, W., Laugwitz, H. J. & Bornfeld, N. Topological relations between the dendrites of olfactory sensory cells and sustentacular cells in different vertebrates. An ultrastructural study. *J. Anat.* **117**, 89–94 (1974).

19. Moran, D. T., Rowley, J. C. & Jafek, B. W. Electron microscopy of human olfactory epithelium reveals a new cell type: the microvillar cell. *Brain Res.* **253**, 39–46 (1982).
20. Cau, E., Casarosa, S. & Guillemot, F. Mash1 and Ngn1 control distinct steps of determination and differentiation in the olfactory sensory neuron lineage. *Dev. Camb. Engl.* **129**, 1871–1880 (2002).
21. Manglapus, G. L., Youngentob, S. L. & Schwob, J. E. Expression patterns of basic helix-loop-helix transcription factors define subsets of olfactory progenitor cells. *J. Comp. Neurol.* **479**, 216–233 (2004).
22. Krolewski, R. C., Packard, A. & Schwob, J. E. Global Expression Profiling of Globose Basal Cells and Neurogenic Progression Within the Olfactory Epithelium. *J. Comp. Neurol.* **521**, (2013).
23. Rodriguez-Gil, D. J. *et al.* Odorant receptors regulate the final glomerular coalescence of olfactory sensory neuron axons. *Proc. Natl. Acad. Sci. U. S. A.* **112**, 5821–5826 (2015).
24. Kondo, K. *et al.* Age-related changes in cell dynamics of the postnatal mouse olfactory neuroepithelium: cell proliferation, neuronal differentiation, and cell death. *J. Comp. Neurol.* **518**, 1962–1975 (2010).
25. Iwema, C. L. & Schwob, J. E. Odorant receptor expression as a function of neuronal maturity in the adult rodent olfactory system. *J. Comp. Neurol.* **459**, 209–222 (2003).
26. Santoro, S. W. & Dulac, C. The activity-dependent histone variant H2BE modulates the life span of olfactory neurons. *eLife* **1**, e00070 (2012).
27. Buck, L. & Axel, R. A novel multigene family may encode odorant receptors: a molecular basis for odor recognition. *Cell* **65**, 175–187 (1991).
28. Barnea, G. *et al.* Odorant receptors on axon termini in the brain. *Science* **304**, 1468 (2004).
29. Schwarzenbacher, K., Fleischer, J. & Breer, H. Formation and maturation of olfactory cilia monitored by odorant receptor-specific antibodies. *Histochem. Cell Biol.* **123**, 419–428 (2005).
30. Belluscio, L., Gold, G. H., Nemes, A. & Axel, R. Mice deficient in G(olf) are anosmic. *Neuron* **20**, 69–81 (1998).
31. Jones, D. T. & Reed, R. R. Golf: an olfactory neuron specific-G protein involved in odorant signal transduction. *Science* **244**, 790–795 (1989).
32. Wong, S. T. *et al.* Disruption of the type III adenylyl cyclase gene leads to peripheral and behavioral anosmia in transgenic mice. *Neuron* **27**, 487–497 (2000).
33. Bakalyar, H. A. & Reed, R. R. Identification of a specialized adenylyl cyclase that may mediate odorant detection. *Science* **250**, 1403–1406 (1990).
34. Dhallan, R. S., Yau, K. W., Schrader, K. A. & Reed, R. R. Primary structure and functional expression of a cyclic nucleotide-activated channel from olfactory neurons. *Nature* **347**, 184–187 (1990).
35. Brunet, L. J., Gold, G. H. & Ngai, J. General anosmia caused by a targeted disruption of the mouse olfactory cyclic nucleotide-gated cation channel. *Neuron* **17**, 681–693 (1996).
36. Ibarra-Soria, X., Levitin, M. O., Saraiva, L. R. & Logan, D. W. The olfactory transcriptomes of mice. *PLoS Genet.* **10**, e1004593 (2014).
37. Clowney, E. J. *et al.* High-throughput mapping of the promoters of the mouse olfactory receptor genes reveals a new type of mammalian promoter and provides insight into olfactory receptor gene regulation. *Genome Res.* **21**, 1249–1259 (2011).
38. Kratz, E., Dugas, J. C. & Ngai, J. Odorant receptor gene regulation: implications from genomic organization. *Trends Genet. TIG* **18**, 29–34 (2002).

39. Rouquier, S. & Giorgi, D. Olfactory receptor gene repertoires in mammals. *Mutat. Res.* **616**, 95–102 (2007).
40. Niimura, Y. & Nei, M. Evolutionary dynamics of olfactory and other chemosensory receptor genes in vertebrates. *J. Hum. Genet.* **51**, 505–517 (2006).
41. Duchamp-Viret, P., Chaput, M. A. & Duchamp, A. Odor Response Properties of Rat Olfactory Receptor Neurons. *Science* **284**, 2171–2174 (1999).
42. Grosmaitre, X. *et al.* SR1, a Mouse Odorant Receptor with an Unusually Broad Response Profile. *J. Neurosci.* **29**, 14545–14552 (2009).
43. Malnic, B., Hirono, J., Sato, T. & Buck, L. B. Combinatorial receptor codes for odors. *Cell* **96**, 713–723 (1999).
44. Nara, K., Saraiva, L. R., Ye, X. & Buck, L. B. A large-scale analysis of odor coding in the olfactory epithelium. *J. Neurosci. Off. J. Soc. Neurosci.* **31**, 9179–9191 (2011).
45. Zhao, H. *et al.* Functional Expression of a Mammalian Odorant Receptor. *Science* **279**, 237–242 (1998).
46. Araneda, R. C., Peterlin, Z., Zhang, X., Chesler, A. & Firestein, S. A pharmacological profile of the aldehyde receptor repertoire in rat olfactory epithelium. *J. Physiol.* **555**, 743–756 (2004).
47. Araneda, R. C., Kini, A. D. & Firestein, S. The molecular receptive range of an odorant receptor. *Nat. Neurosci.* **3**, 1248–1255 (2000).
48. Xu, L. *et al.* Widespread receptor-driven modulation in peripheral olfactory coding. *Science* **368**, (2020).
49. Vassar, R., Ngai, J. & Axel, R. Spatial segregation of odorant receptor expression in the mammalian olfactory epithelium. *Cell* **74**, 309–318 (1993).
50. Ressler, K. J., Sullivan, S. L. & Buck, L. B. A zonal organization of odorant receptor gene expression in the olfactory epithelium. *Cell* **73**, 597–609 (1993).
51. Sullivan, S. L., Ressler, K. J. & Buck, L. B. Odorant receptor diversity and patterned gene expression in the mammalian olfactory epithelium. *Prog. Clin. Biol. Res.* **390**, 75–84 (1994).
52. Tan, L. & Xie, X. S. A Near-Complete Spatial Map of Olfactory Receptors in the Mouse Main Olfactory Epithelium. *Chem. Senses* **43**, 427–432 (2018).
53. Chess, A., Simon, I., Cedar, H. & Axel, R. Allelic inactivation regulates olfactory receptor gene expression. *Cell* **78**, 823–834 (1994).
54. Strotmann, J. *et al.* Local Permutations in the Glomerular Array of the Mouse Olfactory Bulb. *J. Neurosci.* **20**, 6927–6938 (2000).
55. Ishii, T. *et al.* Monoallelic expression of the odourant receptor gene and axonal projection of olfactory sensory neurones. *Genes Cells Devoted Mol. Cell. Mech.* **6**, 71–78 (2001).
56. Tan, L., Li, Q. & Xie, X. S. Olfactory sensory neurons transiently express multiple olfactory receptors during development. *Mol. Syst. Biol.* **11**, 844 (2015).
57. Hanchate, N. K. *et al.* Single-cell transcriptomics reveals receptor transformations during olfactory neurogenesis. *Science* **350**, 1251–1255 (2015).
58. Saraiva, L. R. *et al.* Hierarchical deconstruction of mouse olfactory sensory neurons: from whole mucosa to single-cell RNA-seq. *Sci. Rep.* **5**, 18178 (2015).
59. Mombaerts, P. *et al.* Visualizing an olfactory sensory map. *Cell* **87**, 675–686 (1996).
60. Vassar, R. *et al.* Topographic organization of sensory projections to the olfactory bulb. *Cell* **79**, 981–991 (1994).
61. Wang, F., Nemes, A., Mendelsohn, M. & Axel, R. Odorant receptors govern the formation of a precise topographic map. *Cell* **93**, 47–60 (1998).

62. Feinstein, P. & Mombaerts, P. A contextual model for axonal sorting into glomeruli in the mouse olfactory system. *Cell* **117**, 817–831 (2004).
63. Feinstein, P., Bozza, T., Rodriguez, I., Vassalli, A. & Mombaerts, P. Axon Guidance of Mouse Olfactory Sensory Neurons by Odorant Receptors and the β2 Adrenergic Receptor. *Cell* **117**, 833–846 (2004).
64. Imai, T. & Sakano, H. Odorant receptor gene choice and axonal projection in the mouse olfactory system. *Results Probl. Cell Differ.* **47**, 57–75 (2009).
65. Ressler, K. J., Sullivan, S. L. & Buck, L. B. Information coding in the olfactory system: evidence for a stereotyped and highly organized epitope map in the olfactory bulb. *Cell* **79**, 1245–1255 (1994).
66. Magklara, A. *et al.* An epigenetic signature for monoallelic olfactory receptor expression. *Cell* **145**, 555–570 (2011).
67. Clowney, E. J. *et al.* Nuclear aggregation of olfactory receptor genes governs their monogenic expression. *Cell* **151**, 724–737 (2012).
68. Vassalli, A., Feinstein, P. & Mombaerts, P. Homeodomain binding motifs modulate the probability of odorant receptor gene choice in transgenic mice. *Mol. Cell. Neurosci.* **46**, 381–396 (2011).
69. Rothman, A., Feinstein, P., Hirota, J. & Mombaerts, P. The promoter of the mouse odorant receptor gene M71. *Mol. Cell. Neurosci.* **28**, 535–546 (2005).
70. Wang, S. S., Lewcock, J. W., Feinstein, P., Mombaerts, P. & Reed, R. R. Genetic disruptions of O/E2 and O/E3 genes reveal involvement in olfactory receptor neuron projection. *Dev. Camb. Engl.* **131**, 1377–1388 (2004).
71. Hirota, J. & Mombaerts, P. The LIM-homeodomain protein Lhx2 is required for complete development of mouse olfactory sensory neurons. *Proc. Natl. Acad. Sci. U. S. A.* **101**, 8751–8755 (2004).
72. Monahan, K. *et al.* Cooperative interactions enable singular olfactory receptor expression in mouse olfactory neurons. *eLife* **6**, (2017).
73. Markenscoff-Papadimitriou, E. *et al.* Enhancer interaction networks as a means for singular olfactory receptor expression. *Cell* **159**, 543–557 (2014).
74. Fuss, S. H., Omura, M. & Mombaerts, P. Local and cis effects of the H element on expression of odorant receptor genes in mouse. *Cell* **130**, 373–384 (2007).
75. Serizawa, S. *et al.* Negative feedback regulation ensures the one receptor-one olfactory neuron rule in mouse. *Science* **302**, 2088–2094 (2003).
76. Monahan, K., Horta, A. & Lomvardas, S. LHX2- and LDB1-mediated trans interactions regulate olfactory receptor choice. *Nature* **565**, 448 (2019).
77. Nguyen, M. Q., Zhou, Z., Marks, C. A., Ryba, N. J. P. & Belluscio, L. Prominent roles for odorant receptor coding sequences in allelic exclusion. *Cell* **131**, 1009–1017 (2007).
78. Lewcock, J. W. & Reed, R. R. A feedback mechanism regulates monoallelic odorant receptor expression. *Proc. Natl. Acad. Sci. U. S. A.* **101**, 1069–1074 (2004).
79. Shykind, B. M. *et al.* Gene switching and the stability of odorant receptor gene choice. *Cell* **117**, 801–815 (2004).
80. Shi, Y. *et al.* Histone Demethylation Mediated by the Nuclear Amine Oxidase Homolog LSD1. *Cell* **119**, 941–953 (2004).
81. Lyons, D. B. *et al.* An epigenetic trap stabilizes singular olfactory receptor expression. *Cell* **154**, 325–336 (2013).

82. Zou, D.-J. *et al.* Absence of adenylyl cyclase 3 perturbs peripheral olfactory projections in mice. *J. Neurosci. Off. J. Soc. Neurosci.* **27**, 6675–6683 (2007).
83. Tan, L., Zong, C. & Xie, X. S. Rare event of histone demethylation can initiate singular gene expression of olfactory receptors. *Proc. Natl. Acad. Sci. U. S. A.* **110**, 21148–21152 (2013).
84. Dalton, R. P., Lyons, D. B. & Lomvardas, S. Co-opting the unfolded protein response to elicit olfactory receptor feedback. *Cell* **155**, 321–332 (2013).
85. pubmeddev & al, W. S., et. Transcription factor ATF5 is required for terminal differentiation and survival of olfactory sensory neurons. - PubMed - NCBI. https://www.ncbi.nlm.nih.gov/pubmed/23090999.
86. Harding, H. P. *et al.* Regulated Translation Initiation Controls Stress-Induced Gene Expression in Mammalian Cells. *Mol. Cell* **6**, 1099–1108 (2000).
87. Watatani, Y. *et al.* Stress-induced translation of ATF5 mRNA is regulated by the 5'-untranslated region. *J. Biol. Chem.* **283**, 2543–2553 (2008).
88. Saito, H., Kubota, M., Roberts, R. W., Chi, Q. & Matsunami, H. RTP family members induce functional expression of mammalian odorant receptors. *Cell* **119**, 679–691 (2004).
89. Scholz, P. *et al.* Transcriptome Analysis of Murine Olfactory Sensory Neurons during Development Using Single Cell RNA-Seq. *Chem. Senses* **41**, 313–323 (2016).
90. Jolma, A. *et al.* DNA-binding specificities of human transcription factors. *Cell* **152**, 327–339 (2013).
91. Rodríguez-Martínez, J. A., Reinke, A. W., Bhimsaria, D., Keating, A. E. & Ansari, A. Z. Combinatorial bZIP dimers display complex DNA-binding specificity landscapes. *eLife* **6**, (2017).
92. Von Dannecker, L. E. C., Mercadante, A. F. & Malnic, B. Ric-8B promotes functional expression of odorant receptors. *Proc. Natl. Acad. Sci. U. S. A.* **103**, 9310–9314 (2006).
93. Von Dannecker, L. E. C., Mercadante, A. F. & Malnic, B. Ric-8B, an olfactory putative GTP exchange factor, amplifies signal transduction through the olfactory-specific G-protein Galphaolf. *J. Neurosci. Off. J. Soc. Neurosci.* **25**, 3793–3800 (2005).
94. Sharma, R. *et al.* Olfactory receptor accessory proteins play crucial roles in receptor function and gene choice. *eLife* **6**, (2017).
95. Machado, C. F. *et al.* Conditional Deletion of Ric-8b in Olfactory Sensory Neurons Leads to Olfactory Impairment. *J. Neurosci. Off. J. Soc. Neurosci.* **37**, 12202–12213 (2017).
96. Khetchoumian, K. *et al.* TIF1δ, a Novel HP1-interacting Member of the Transcriptional Intermediary Factor 1 (TIF1) Family Expressed by Elongating Spermatids. *J. Biol. Chem.* **279**, 48329–48341 (2004).
97. Manterola, M. *et al.* BRDT is an essential epigenetic regulator for proper chromatin organization, silencing of sex chromosomes and crossover formation in male meiosis. *PLOS Genet.* **14**, e1007209 (2018).
98. Kagey, M. H., Melhuish, T. A. & Wotton, D. The polycomb protein Pc2 is a SUMO E3. *Cell* **113**, 127–137 (2003).
99. Blais, J. D. *et al.* Activating transcription factor 4 is translationally regulated by hypoxic stress. *Mol. Cell. Biol.* **24**, 7469–7482 (2004).
100. Saito, A. *et al.* Endoplasmic reticulum stress response mediated by the PERK-eIF2(alpha)-ATF4 pathway is involved in osteoblast differentiation induced by BMP2. *J. Biol. Chem.* **286**, 4809–4818 (2011).
101. Gachon, F. *et al.* The cAMP response element binding protein-2 (CREB-2) can interact with the C/EBP-homologous protein (CHOP). *FEBS Lett.* **502**, 57–62 (2001).

102. Vallejo, M., Ron, D., Miller, C. P. & Habener, J. F. C/ATF, a member of the activating transcription factor family of DNA-binding proteins, dimerizes with CAAT/enhancer-binding proteins and directs their binding to cAMP response elements. *Proc. Natl. Acad. Sci. U. S. A.* **90**, 4679–4683 (1993).
103. Bakker, O. & Parker, M. G. CAAT/enhancer binding protein is able to bind to ATF/CRE elements. *Nucleic Acids Res.* **19**, 1213–1217 (1991).
104. Huggins, C. J. *et al.* C/EBPγ Is a Critical Regulator of Cellular Stress Response Networks through Heterodimerization with ATF4. *Mol. Cell. Biol.* **36**, 693–713 (2015).
105. Huggins, C. J. *et al.* C/EBPγ suppresses senescence and inflammatory gene expression by heterodimerizing with C/EBPβ. *Mol. Cell. Biol.* **33**, 3242–3258 (2013).
106. Shimizu, Y. I. *et al.* Fasting induced up-regulation of activating transcription factor 5 in mouse liver. *Life Sci.* **84**, 894–902 (2009).
107. Nakano, H. *et al.* Co-expression of C/EBPγ and ATF5 in mouse vomeronasal sensory neurons during early postnatal development. *Cell Tissue Res.* (2019) doi:10.1007/s00441-019-03070-2.
108. Mardaryev, A. N. *et al.* Cbx4 maintains the epithelial lineage identity and cell proliferation in the developing stratified epithelium. *J. Cell Biol.* **212**, 77–89 (2016).
109. Polycomb Cbx family members mediate the balance between haematopoietic stem cell self-renewal and differentiation | Nature Cell Biology. https://www.nature.com/articles/ncb2701.
110. Howard, P. W., Jue, S. F., Ransom, D. G. & Maurer, R. A. Regulation of LIM-Domain-Binding 1 Protein Expression by Ubiquitination of Lysine-134. *Biochem. J.* **429**, 127–136 (2010).
111. Howard, P. W., Ransom, D. G. & Maurer, R. A. Transcription intermediary factor 1gamma decreases protein expression of the transcriptional cofactor, LIM-domain-binding 1. *Biochem. Biophys. Res. Commun.* **396**, 674–678 (2010).
112. Greenwood, M., Greenwood, M. P., Paton, J. F. R. & Murphy, D. Transcription Factor CREB3L1 Regulates Endoplasmic Reticulum Stress Response Genes in the Osmotically Challenged Rat Hypothalamus. *PloS One* **10**, e0124956 (2015).
113. Saito, A., Hino, S.-I., Murakami, T., Kondo, S. & Imaizumi, K. A novel ER stress transducer, OASIS, expressed in astrocytes. *Antioxid. Redox Signal.* **9**, 563–571 (2007).
114. Nakano, H. *et al.* Activating transcription factor 5 (ATF5) is essential for the maturation and survival of mouse basal vomeronasal sensory neurons. *Cell Tissue Res.* **363**, 621–633 (2016).
115. Pascual, M., Gómez-Lechón, M. J., Castell, J. V. & Jover, R. ATF5 Is a Highly Abundant Liver-Enriched Transcription Factor that Cooperates with Constitutive Androstane Receptor in the Transactivation of CYP2B6: Implications in Hepatic Stress Responses. *Drug Metab. Dispos.* **36**, 1063–1072 (2008).
116. Du, Y. *et al.* Human Hepatocytes with Drug Metabolic Function Induced from Fibroblasts by Lineage Reprogramming. *Cell Stem Cell* **14**, 394–403 (2014).
117. Nakamori, D. *et al.* Hepatic maturation of human iPS cell-derived hepatocyte-like cells by ATF5, c/EBPα, and PROX1 transduction. *Biochem. Biophys. Res. Commun.* **469**, 424–429 (2016).
118. Angelastro, J. M. *et al.* Regulated Expression of ATF5 Is Required for the Progression of Neural Progenitor Cells to Neurons. *J. Neurosci.* **23**, 4590–4600 (2003).

119. Angelastro, J. M. *et al.* Downregulation of Activating Transcription Factor 5 Is Required for Differentiation of Neural Progenitor Cells into Astrocytes. *J. Neurosci.* **25**, 3889–3899 (2005).
120. Lee, H. Y., Angelastro, J. M., Kenney, A. M., Mason, C. A. & Greene, L. A. Reciprocal actions of ATF5 and Shh in proliferation of cerebellar granule neuron progenitor cells. *Dev. Neurobiol.* **72**, (2012).
121. Mason, J. L. *et al.* ATF5 regulates the proliferation and differentiation of oligodendrocytes. *Mol. Cell. Neurosci.* **29**, 372–380 (2005).
122. Hettmann, T., Barton, K. & Leiden, J. M. Microphthalmia due to p53-mediated apoptosis of anterior lens epithelial cells in mice lacking the CREB-2 transcription factor. *Dev. Biol.* **222**, 110–123 (2000).
123. Tanaka, T. *et al.* Targeted disruption of ATF4 discloses its essential role in the formation of eye lens fibres. *Genes Cells Devoted Mol. Cell. Mech.* **3**, 801–810 (1998).
124. Zhao, Y. *et al.* ATF4 plays a pivotal role in the development of functional hematopoietic stem cells in mouse fetal liver. *Blood* **126**, 2383–2391 (2015).
125. Masuoka, H. C. & Townes, T. M. Targeted disruption of the activating transcription factor 4 gene results in severe fetal anemia in mice. *Blood* **99**, 736–745 (2002).
126. Peters, C. S. *et al.* ATF-7, a Novel bZIP Protein, Interacts with the PRL-1 Protein-tyrosine Phosphatase. *J. Biol. Chem.* **276**, 13718–13726 (2001).
127. Torres-Peraza, J. F. *et al.* Protective neuronal induction of ATF5 in endoplasmic reticulum stress induced by status epilepticus. *Brain J. Neurol.* **136**, 1161–1176 (2013).
128. Hernández, I. H. *et al.* The neuroprotective transcription factor ATF5 is decreased and sequestered into polyglutamine inclusions in Huntington's disease. *Acta Neuropathol. (Berl.)* **134**, 839–850 (2017).
129. Zhu, P. J. *et al.* Activation of the ISR mediates the behavioral and neurophysiological abnormalities in Down syndrome. *Science* **366**, 843–849 (2019).